Chapter 6

Thermal and Transport properties of Chromium Alloys

6.1 Introduction

Pure Chromium is antiferromagnetic below 311 K. Above this temperature, known as the Neel temperature, it transforms to a paramagnetic phase. The antiferromagnetism of Chromium (Cr) has some unique features. It is an itinerant spin-density wave antiferromagnet, i.e, the antiferromagnetism is due to itinerant or conduction electrons. Therefore the magnetic moments are not localized at the atomic sites. Paramagnetic neutron scattering studies on isotopically enriched specimens have shown that there exist no localized moments in Chromium above the Neel temperature [1].

A unique feature of the spin-density wave in Chromium is that the wave-vector is incommensurate with the lattice, i.e, if $\vec{q}$ is the wave-vector for the spin-density wave, then $\vec{q}$ has the value

$$\vec{q} = \pm(2\pi/a)(1 - \delta_o, 0, 0) \tag{6.1}$$

in terms of the lattice translation vectors. Here δ_o is a temperature dependent quantity between 0.05 and 0.035. Hence the spin-density wave is almost on the verge of becoming commensurate.

The presence of a lattice makes $\vec{q} + \vec{G}$ (where $\vec{G}$ is a reciprocal lattice vector) an equivalent representation of $\vec{q}$. Consequently, the spin-density wave (SDW) can also be defined , for instance by

$$\vec{q} = \pm(2\pi/a)(1 + \delta_o, 0, 0) \tag{6.2}$$

From the above equations, it is evident that the spin-density wave exists only

in the (100) plane.

The origin of the incommensurate spin-density wave in Cr was recognized by Overhauser [2] to be the nesting electron and hole Fermi surfaces. The electron and hole Fermi surfaces in the (100) plane are shown in Fig 6.1.

As seen from the figure , the wave-vector $\vec{q}$ connects , two 'flat' pieces of the so-called hole octahedron and electron-jack. The flat portions of the Fermi surface are crucial for the occurrence of magnetic order, because the direction of magnetization is the same for a large portion of the Fermi surface. The portions of the Fermi surface which are more free-electron like (spherical) do not contribute to the antiferromagnetic ordering as the direction of the SDW is different at each point . The flat portions of the Fermi surface are the d-like states while the 'knobs', which are spherical in shape correspond to the s-like electrons. Since the d-like states are flat they have a larger surface area and hence can accommodate more number of states. This is the origin of the fact that the d-states have a higher density of states at the Fermi level when compared to the s-states. Also because of this flat nature of the Fermi surface, $d\epsilon/dk$ at ϵ_f (which is equal to the velocity of the electrons at the Fermi surface), is quite small. Therefore the electrical conduction is mainly due to the s-like portions of the Fermi surface. Moreover, the d-states reduce the conductivity by providing states to which the s-electrons can be scattered into by phonons.

The interaction between the electrons and the holes which are connected by $\vec{q}$ leads to a gap in the energy spectrum. If the paramagnetic energy spectrum of the electrons is described by a band structure $\epsilon(k)$, the antiferromagnetic energy spectrum has gaps whenever the condition

$$\epsilon(\vec{k}) = \epsilon(\vec{k} + n\vec{q}) \tag{6.3}$$

is satisfied. n is any non-zero integer.

It has been proven experimentally and theoretically that values of the gaps with $n \neq 1$ are in general very small and can be neglected. Consequently above equation reduces to

$$\epsilon(\vec{k}) = \epsilon(\vec{k} \pm \vec{q}) \tag{6.4}$$

The magnitude of these antiferromagnetic gaps is proportional to M_q, where M_q is the magnetization.

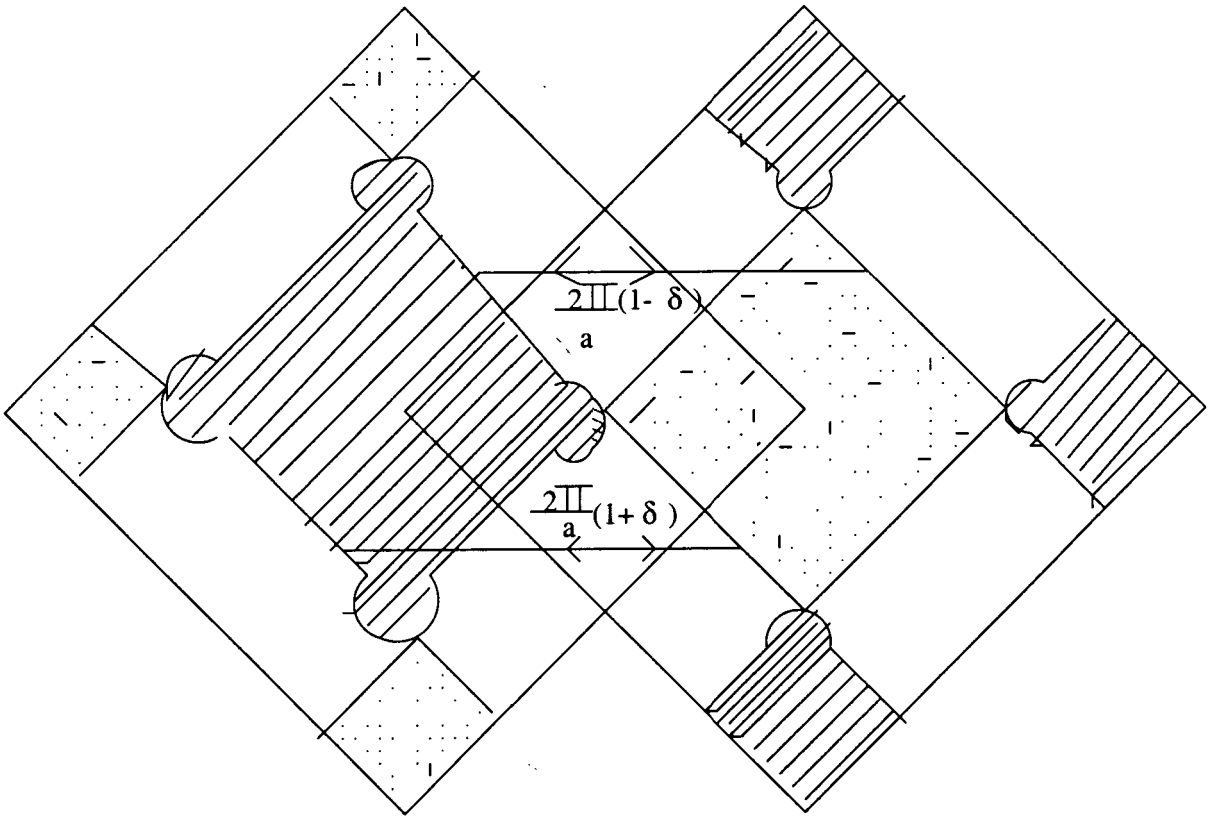

Key :

Electrons

Holes

Figure 6.1: The Fermi surface of Chromium showing the electron and hole sheets and the wave-vectors connecting them **[3]**

Due to the appearance of the energy gaps, considerable portions of the Fermi surface are annihilated , i.e, the density of states in those portions is zero.

The reduction in the density of states at the Fermi energy in turn reduces the conductivity. Mcwhan and Rice [4] have calculated the reduction in the conductivity due to the electron-hole condensation in the nesting octahedra. They divided the conductivity into two components, $a,$ and $a_{,,}$ where σ_r comes from the noncondensing reservoir and σ_n from the nesting parts of the Fermi surface that condense to form electron-hole pairs.

Thus $a,$ is unaffected by the condensation, with $a, = \sigma_{rp}$ at all temperatures T , whereas the conductivity σ_n in the AFM phase is decreased relative to the conductivity σ_{np} at the same temperature, extrapolated from the paramagnetic phase in the ratio

$$\frac{\sigma_n}{\sigma_{np}} = \int_{-\infty}^{+\infty} \frac{\Delta^2}{(E^2+\Delta^2)^{3/2}} \frac{dE}{exp[(E^2+\Delta^2)^{1/2}/k_BT]+1} \tag{6.5}$$

where $2\Delta(T)$ is the temperature-dependent energy gap.

Since resistivity is the quantity which is usually measured in experiments, the reduction in the conductivity is seen as a corresponding increase in the resistivity. The increase of the resistivity in comparison to the linear extrapolation from the paramagnetic phase is given by:

$$\frac{\Delta R}{R}(T) = \frac{R - R_p}{R} \tag{6.6}$$

where $R_p(T)$ is a linear extrapolation into the SDW phase of the resistivity in the paramagnetic phase.

The resistivity defined above is related to the reduction in conductivity by the following expression:

$$\frac{\Delta R}{R} = g\frac{\sigma_{np}}{\sigma_p} \tag{6.7}$$

Where

$$g = \frac{\sigma_{np} - \sigma_n}{\sigma_{np}} = 1 - \frac{\sigma_n}{\sigma_{np}} \tag{6.8}$$

is the fraction of the nesting octahedra that condenses, and

$$\frac{\sigma_{np}}{\sigma_p} = \frac{\sigma_{np}}{\sigma_r + \sigma_{np}} \tag{6.9}$$

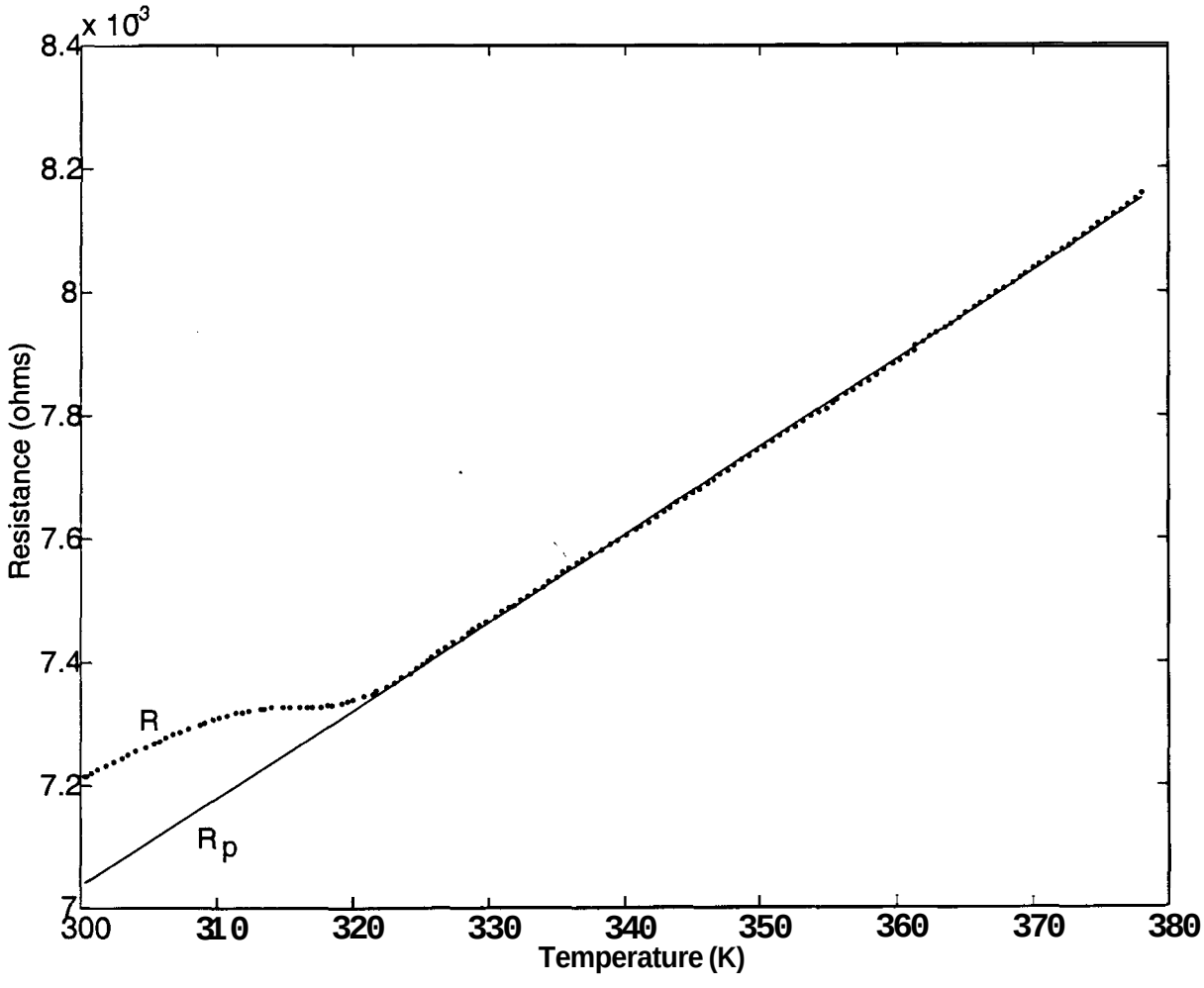

Figure 6.2: Resistivity of $Cr_{0.995}Re_{0.005}$ as a function of temperature. The solid line is the linear extrapolation from the paramagnetic phase into the antiferromagnetic (AFM) phase

---

is the fraction of the total Fermi surface in the octahedra.

In the calculations to be described in the next section, this fraction has been taken to be 0.3. This is the approximate figure for pure Chromium [5]. This fraction might change with alloying or with pressure [4]. However since there is no data available to take into account these effects, we assume this fraction to be a constant for all pressures and compositions. Obviously, this will introduce systematic errors in the calculation of various quantities.

Fig. 6.2 shows the variation in the resistivity for the alloy $Cr_{0.995}Re_{0.005}$ near its Neel temperature. It is seen from the figure that the resistivity in the AFM phase (R) is higher than the linear extrapolation (R_p) of the resistance from the

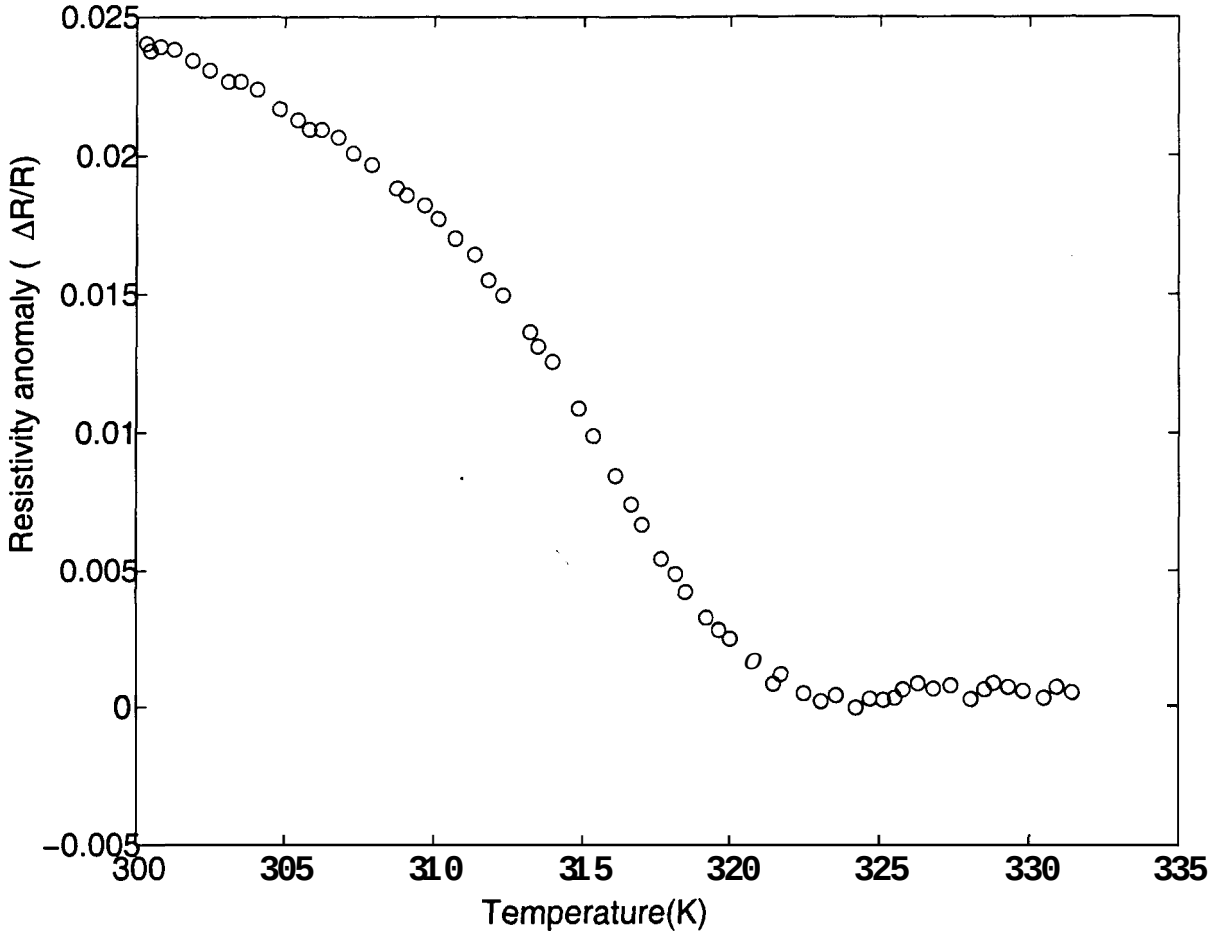

Figure 6.3: The resistivity anomaly (defined by equation 6.6) for $Cr_{0.995}Re_{0.005}$ as a function of temperature.

paramagnetic phase. This increase in the resistivity in the AFM phase is shown in Fig. 6.3.

The antiferromagnetic state in Cr is clearly critically dependent on the electronic band structure and therefore it is of interest to study the change in the magnetic properties as the electronic structure is changed. The electronic structure of Chromium can be changed by alloying. If Chromium is alloyed with Mn, Tc, Ru, Rh and Re, the electron to atom (e/a) ratio and hence the Neel temperature and the magnetic moment are increased. If Cr is alloyed with V, Nb or Ta, the e/a ratio and the Neel temperature decrease. This can be understood in a simple manner. Let us consider the case when Cr is alloyed with Re. While the electronic configuration of Cr is $3d^5 4s'$, the configuration of Re is $5d^5 6s^2$. Hence, electrons are introduced into the system, this increases the number of electron-hole pairs, as initially the number

of holes is greater than the number of electrons. The Neel temperature will continue to increase till a limit when any further increase in the number of electrons will lead to an excess of electrons as compared to holes. Beyond this the Neel temperature will start to decrease [6]. The injection of electrons into the system will also increase the wave-vector $\vec{q}$ as the electron jack has increased in size. This will reduce δ. With increasing concentration of Re, δ will reduce continuously, untill at a concentration of around 0.4 % Re [5], the SDW becomes commensurate with the lattice. The phase diagrams for different Cr alloys, showing the commensurate and incommensurate AFM phases has been experimentally determined by various workers [7].The SDW remains 'locked' to the reciprocal lattice vector for even higher concentrations of Re. The SDW remains commensurate except for the highest Re concentrations.

For very high concentrations of Re, $\vec{q}$ no longer 'follows' the Fermi surface. while the Fermi energy goes on increasing with increasing electron concentration, the wave-vector remains 'locked' to the reciprocal lattice vector. This means that there is little mutual annihilation of the Fermi surface on magnetic ordering. The states near the Fermi surface are relatively little affected. In such a situation the resistivity is mainly due to superzone plane boundaries which cut the Fermi surface. A superzone plane which cuts the Fermi surface causes a resistance change $(\frac{\Delta\rho}{\rho})$ proportional to the magnetic moment.

Hence it is seen that the explanation of the transport properties depends on whether we are dealing with a commensurate SDW or an incommensurate SDW.

Another convenient way of changing the electronic structure is by the application of pressure. Pressure is found to have an effect which is analogous to decreasing electron concentration [7]. A combination of alloying and pressure has also been tried by various workers. The effect of pressure on Cr alloy systems has been studied for a number of solutes, since the atomic volume is a fundamental parameter whose effect on the magnetic properties should give considerable physical insight.

We have studied the thermal and transport properties of $Cr_{0.995}Re_{0.005}$ and $Cr_{0.99}Re_{0.01}$ as a function of temperature as well as pressure.

6.2 Resistivity studies for $Cr_{0.995}Re_{0.005}$ and $Cr_{0.99}Re_{0.01}$ alloys

6.2.1 Experimental

Chromium alloys were prepared by arc melting and homogenized at 1200' C and then furnace cooled. The resistivity studies were carried out using an ac 4-probe technique, which is described in detail in chapter 2.

The high pressure experiments were carried out in a Teflon cell (Fig. 2.4) using a piston-cylinder apparatus. Silicone oil was used as the pressure transmitting medium. The high pressure resistivity runs were performed by keeping the pressure at a constant value and varying the temperature.

The entire experimental arrangement, including the lock-in amplifier was interfaced to a personal computer using the IEEE 488.2 interface. The temperature of the sample was read using a Keithley 2001 multimeter. The sample temperature can be controlled to an accuracy of $\pm 0.05C$ using a PID algorithm implemented in the software. The sample is heated by a small disk shaped heater which is placed just below the sample. The heat is conducted to the sample through the oil. The resistance of the sample was measured at intervals of 0.5^oC and stored in a file.

6.2.2 Resistivity results on $Cr_{0.995}Re_{0.005}$ alloy

The resistance of $Cr_{0.995}Re_{0.005}$ is shown as a function of temperature at different pressures in Fig. 6.4.

Fig. 6.4 shows the resistance at 0.2,0.5, 1,2,3 and 10 kbars. Except for the run at 500 bars, all the other runs show the normal trend of decreasing resistance with increase in pressure. The resistance in the paramagnetic phase is quite linear. This is due to the fact that this is in the region near the Debye temperature (θ_D), which is 630 k for pure Chromium. It is only below $\theta_D/4$ that non-linearities in the resistivity due to the temperature dependent electron-phonon scattering become apparent [9]. The antiferromagnetic transition is seen as a flattening of the resistance. The Neel temperature is usually identified as the temperature at which $d\rho/dT$ is a minimum. This procedure is convenient if the anti-ferromagnetic transition manifests itself as a 'hump', i.e., an increase in the resistivity below the Neel temperature. Such a 'hump' is clearly seen in the work of Arajs [6]. This 'hump' becomes more prominent at higher concentrations of Re. However for the low concentrations of Re which we have worked with, there is no actual 'hump', only a flattening of the curve

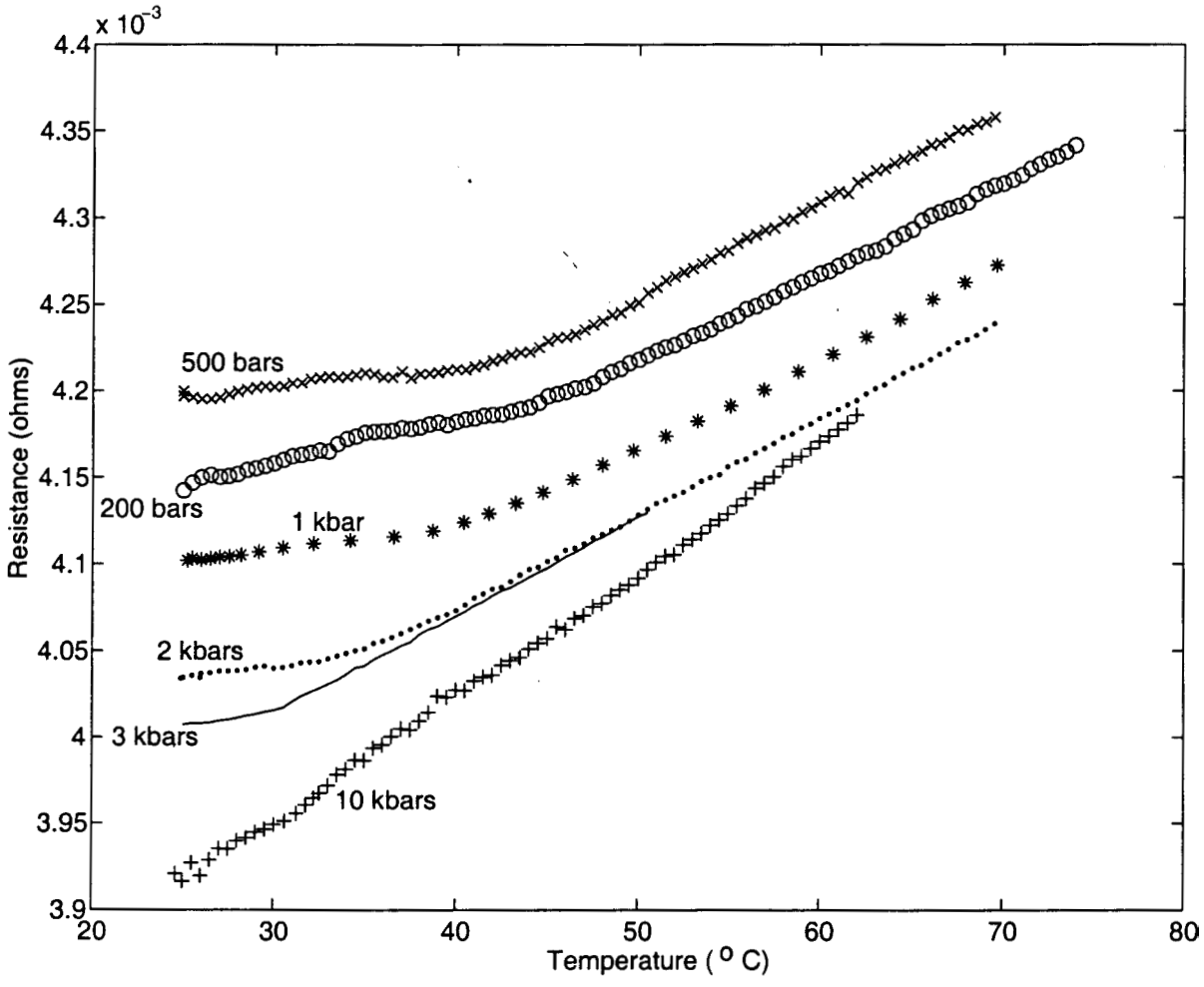

Figure 6.4: The resistance of $Cr_{0.995}Re_{0.005}$ as a function of temperature at different pressures

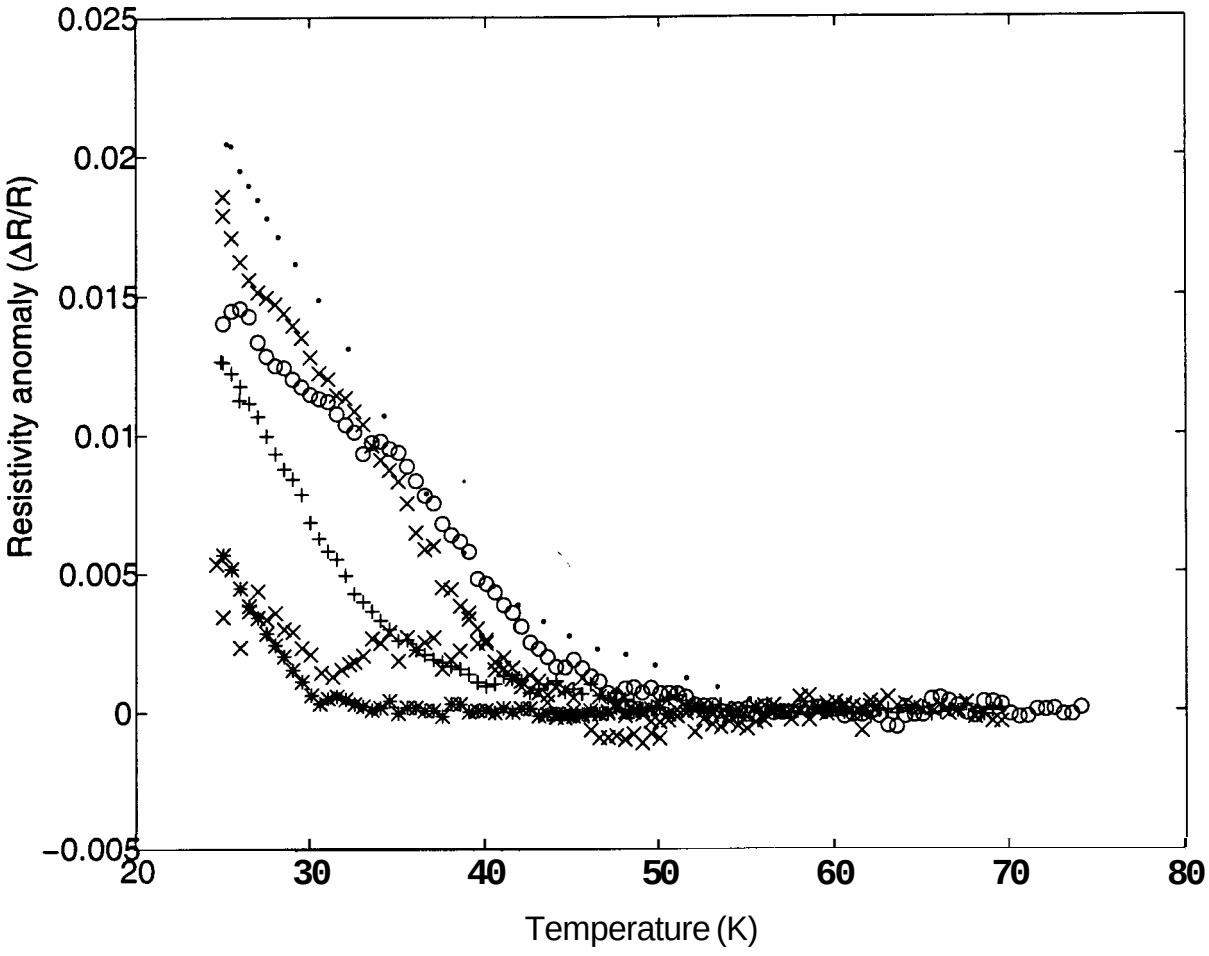

Figure 6.5: The resistivity anomaly in $Cr_{0.995}Re_{0.005}$ at different pressures. Key:'o'- 200 bars, 'x'- 500 bars, '.' - 1 kbar, '+'- 2 kbar, '*'- 3 kbar, 'X'- 10 kbar

near the Neel temperature. In these cases, a more reliable identification of the Neel temperature can be achieved by using the resistivity anomaly (see Fig. 6.3). The Neel temperature is identified as the temperature at which the resistivity anomaly becomes zero. However even this procedure is not fool-proof in practice, as it is found that the resistivity anomaly does not become exactly zero at the Neel temperature. This is due to the fact the some magnetic order persists well above the Neel temperature. This persistence of magnetic order above the Neel temperature has been observed using Neutron scattering.

From the resistivity anomaly it is possible to calculate the value of the energy gap which gives rise to this anomaly. The procedure for calculating the value of the energy gap at 0 k as also the identification of the Neel temperature is given in the

next section.

6.2.3 Calculation ofthezero temperatureenergygap

The zero temperature energy gap is calculated by the following procedure:

1) Assume some value for the energy gap which is almost zero.

2)Evaluate the value of g corresponding to this value of A.

3)Calculate the corresponding value of the resistivity anomaly.

4) Calculate the difference between the experimental and theoretical values of the resistivity anomaly.

5) Iteratively calculate the value of A which minimizes this difference. This gives the value of A for that temperature.

6) This procedure is repeated for all 'the temperatures for which the experimental data is available.

7) From this a curve of A as a function of temperature is generated.

This procedure is slightly different from that of Mcwhan and Rice [4] who assumed that the energy gap obeys an equation similar to a superconductor, i.e, the exponent β in Eq. 6.10 is 0.5. We have tried to arrive at the value of β using the resistivity data.

We are able to fit an equation of the form

$$\Delta(T) = \Delta(0)\left(\frac{T_n - T}{T_n}\right)^{\beta} \tag{6.10}$$

The fit is performed by using a least squares fit on a log-log plot as shown in Fig. 6.6.

Since the energy gap can be considered as the order parameter for this transition. the exponent describing the temperature variation of A is the order parameter exponent β.

The values of β and Neel temperature obtained by this fitting procedure is given in the table below:

The temperature variation of the energy gap is shown in Figure 6.7 for 3 different pressures. As is seen from the graph, the temperature variation of the energy gap seems to follow the nature of the resistivity anomaly.

This is not surprising if we analyze Equation 6.5 a little carefully. The integrand of Eq. 6.5 is shown in Fig. 6.8

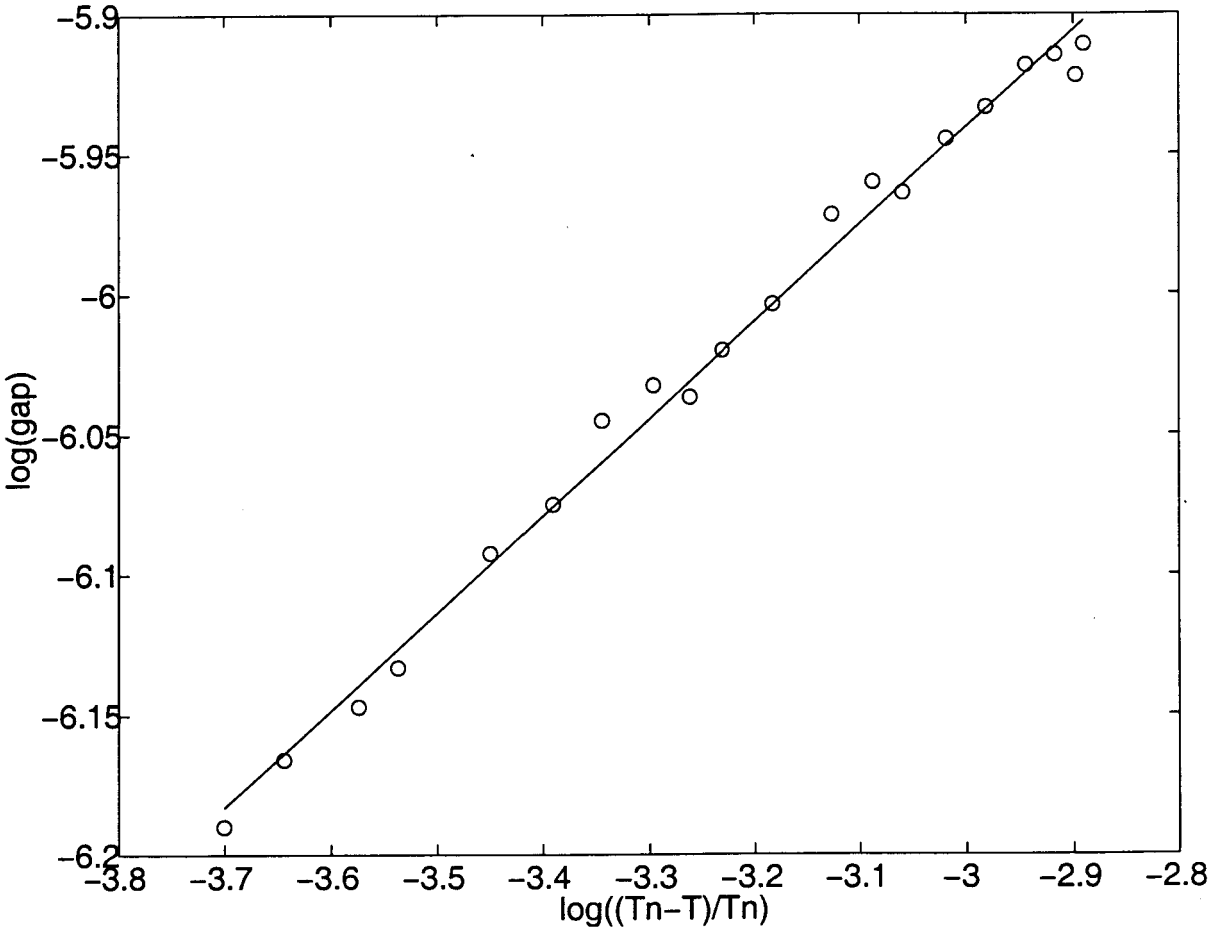

Figure 6.6: A log-log plot of Eq. 6.10. The solid line is a least squares fit to the data.

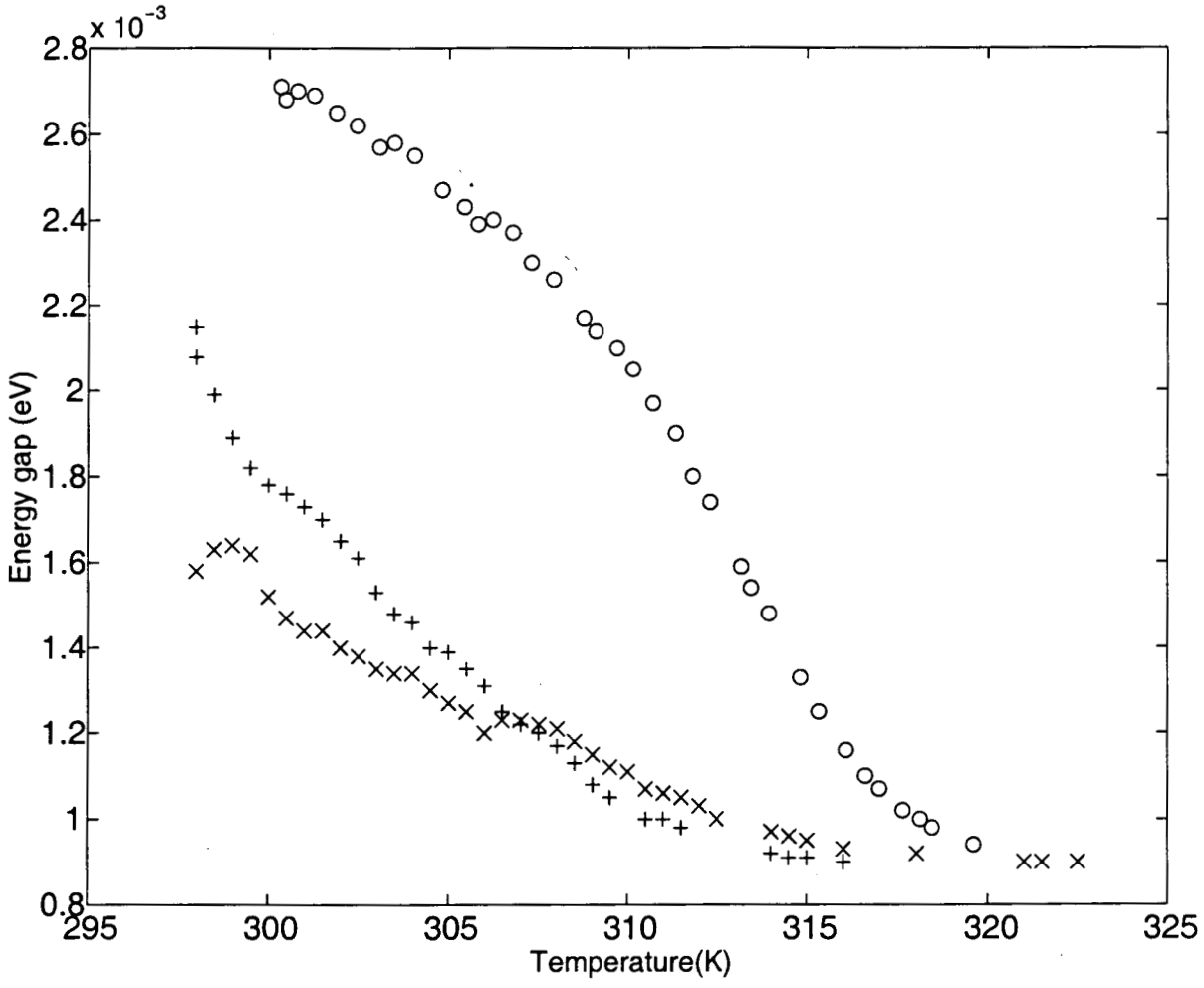

Figure 6.7: Variation of the energy gap with temperature. Key:- 'o'- 1 bar,'+'- 500 bars. 'x' - 200 bars

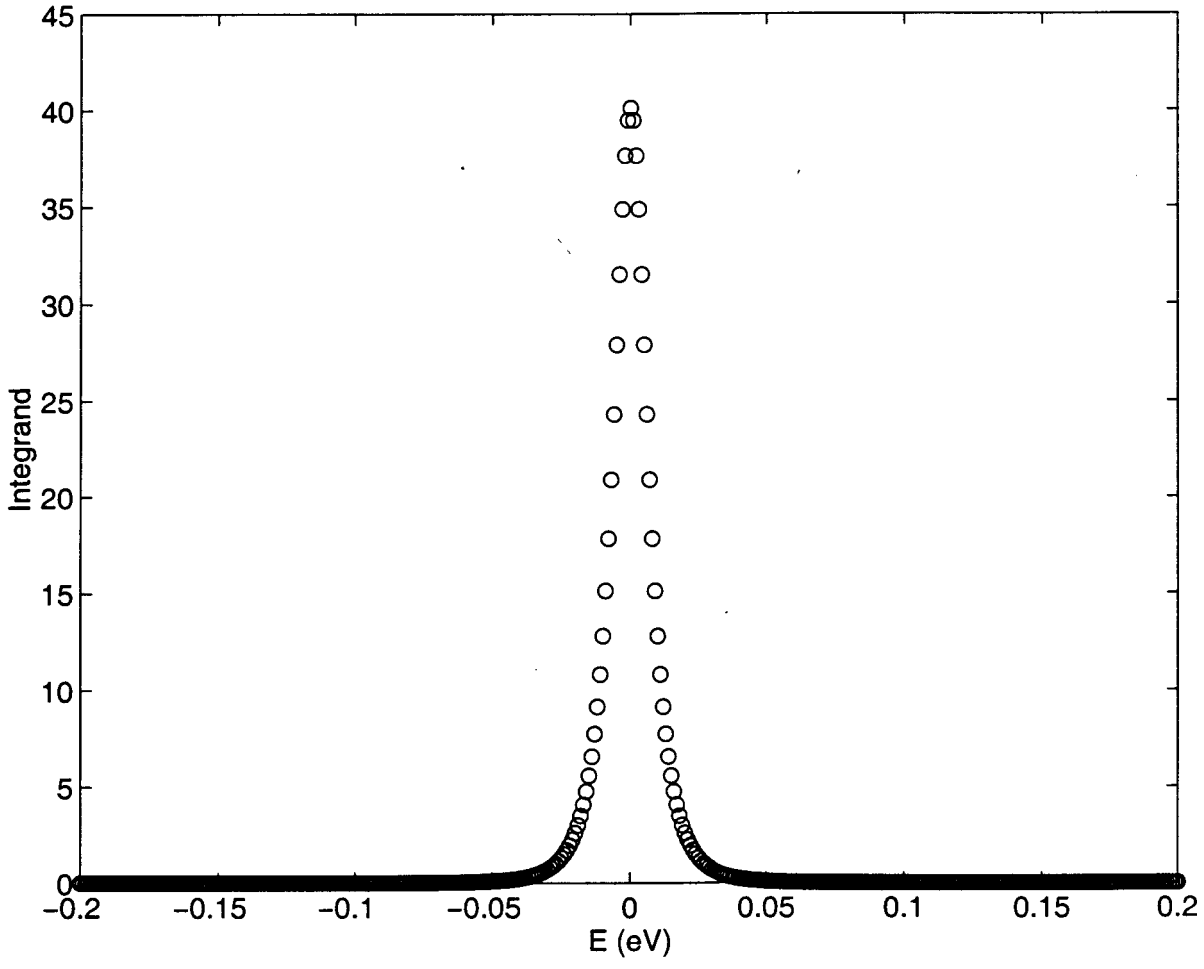

Figure 6.8: The integrand in Equation 6.5 as a function of the energy in electron volts

Table 6.1: Pressure dependence of the Neel temperature and the energy gap in $Cr_{0.995}Re_{0.005}$

Pressure	Neel temperature	Energy gap (0 k)	Δ (0)/kT	β
1 bar	318 k	0.015 eV	0.55	0.38
200 bars	316 k	0.0072 eV	0.27	0.52
500 bars	312 k	0.0078 eV	0.029	0.45
1 kbar	305 k	-	-	-
2 kbar	302 k	-	-	-
3 kbar	300.5 k	-	-	-

As is evident from the figure, most of the contribution to the integral comes from the region near E=0. Hence we can approximate the integral to a/Δ near E=0, under the assumption that A $<<$ kT. Hence the resistivity anomaly is given by:

$$\frac{\Delta R}{R} = \left(1 - \frac{a}{\Delta}\right) \frac{\sigma_{np}}{\sigma_p} \tag{6.11}$$

Here 'a' is some constant having the dimensions of energy. Hence it is seen that the resistivity anomaly increases in magnitude as the magnitude of the energy gap increases.

In calculating the value of the energy gaps and in the determination of the exponent β, we have neglected data points which are very close to T_N as these do not seem to fit into Equation 6.10. This is because of the persistence of the magnetic order even above the Neel temperature. The Neel temperature is determined after neglecting these points. The Neel temperature is taken as that temperature at which the extrapolated resistivity anomaly becomes zero.

It was not possible to calculate the values of the energy gap and the exponent β for pressures above 500 bars, as the number of experimental points are very less in these cases. In the experimental arrangement available, it is only possible to make measurements above room temperature. Since the Neel temperature decreases with increase in pressure, the number of data points available for analysis reduces drastically at higher pressures.

As expected the energy gap reduces with pressure.

According to the two-band theory of Fedders and Martin [10], the ratio of the zero-temperature energy gap and the Neel temperature T_N is given by:

$$\frac{\Delta(0)}{kT_N} = \frac{\pi v}{\gamma_e v*} \tag{6.12}$$

Where v is the arithmetic mean ($\frac{1}{2}(v_e + v_h)$) and $v*$ is the geometric mean of the electron and hole velocities at the Fermi surface. γ is the mean overlap matrix element for electrons in the same band.

In the theory of Fedders and Martin, $\gamma_e = 1.78$, so that

$$\frac{\Delta(0)}{kT_N} = 1.76\left(\frac{v}{v*}\right) \tag{6.13}$$

From experiments on pure Chromium, it is found that

$$\frac{\Delta(0)}{kT_N} = 2.2 \tag{6.14}$$

Since v must be greater than or equal to $v*$, in the case of pure Chromium there seems to be good agreement between theory and experiment.

According to the two-band model,

$$g = \pi k_B T_N (8v^2/7\pi^2\xi(3))^{1/2}\left[1 - (T/T_N)\right]^{1/2}\Big] \tag{6.15}$$

where $\zeta(3)$ is the Reimann-Zeta function with argument **3.** This gap varies with temperature as in a superconductor. Neutron-diffraction experiments seem to verify that this is the general shape of the gap although they give a small tail which goes past T_N. The effects of the tail mentioned above are also seen in our resistivity data. This tail is only **3%** of the total intensity (in neutron diffraction experiments) for single crystals of Cr but becomes significantly larger for more finely granulated samples. From our resistivity measurements , it is seen that the 'tail' becomes more and more prominent at higher pressures.

From Eq. 6.13, it is seen that the ratio $\frac{\Delta(0)}{kT_N}$ depends only on the ratio $v/v*$. The variation of $v/v*$ with increasing electron concentration is shown in Fig. 6.9. The x-axis in the figure is for relative electron concentration, i.e, when the electron concentration is equal to 1 in the figure, it signifies a band completely filled with electrons and 0 is a band with no electrons. It is seen that when the electron concentration is almost equal to the hole concentration, the ratio $v/v*$ and hence $\Delta(0)/kT_n$, does not vary much with change in electron concentration. The ratio $v/v*$, has been calculated using the fact that electron velocity is proportional to (electron concentration)$^{1/3}$. The difference in mobility of electrons and holes has not been taken into account in this calculation.

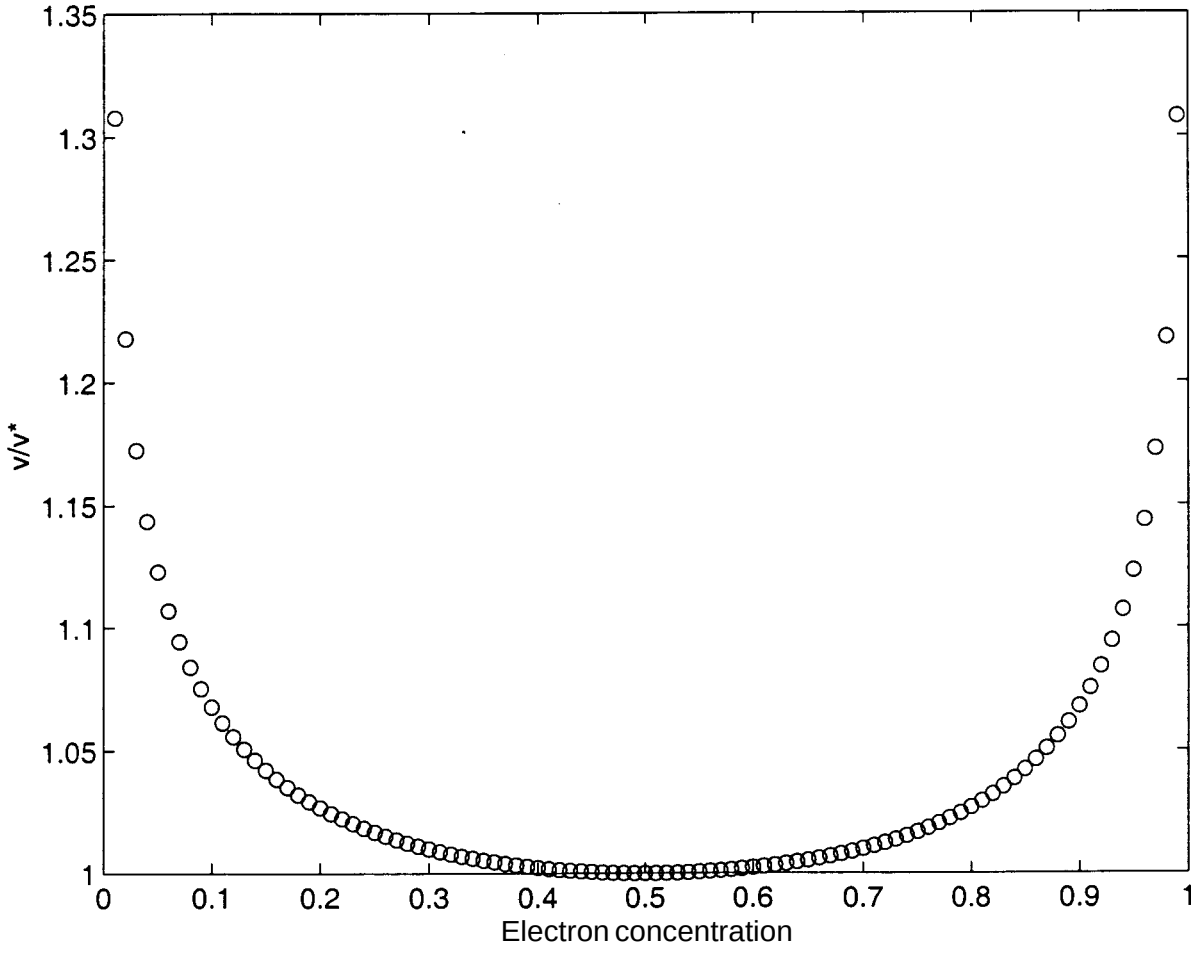

Figure 6.9: Variation of the ratio $v/v*$ with change in the relative concentration of electrons and holes.

From our resistivity measurements, it is seen that the ratio $\Delta(0)/kT_N$, decreases with pressure. Also the decrease in the value of $\Delta(0)/kT_N$ for $Cr_{0.995}Re_{0.005}$ compared to the value for pure Cr can be understood from Fig. 6.9. Alloying with Re increases the concentration of electrons and increasing the electron concentration initially leads to a decrease in $v/v*$ and consequently a decrease in $\Delta(0)/kT_N$.

According to Eq. 6.15, the value of β should be 0.5. From the data for $Cr_{0.995}Re_{0.005}$, it is seen that for some of the cases, the value of β obtained is less than 0.5. It has to be borne in mind that the theory of Fedders and Martin is not an exact one and the exact theory could have an exponent different from 0.5. Eq. 6.5 is derived under the assumption that the change in conductivity is only due to a change in the number of charge carriers. However there will also be a change in the relaxation time, due to the change in the density of states available for the scattered electrons. Another factor which could lead to a correction is that at temperatures lesser than $\theta_D/2$, the number of phonons will reduce and consequently the scattering of electrons by phonons will also reduce. The predominant factor which affects the behaviour of the conductivity can only be known after a detailed analysis of the data after taking into account all these factors. Since the number of data points for the $Cr_{0.995}Re_{0.005}$ sample is less, such an analysis has been carried out only for the $Cr_{0.99}Re_{0.01}$ sample.

6.2.4 Variation of T_N with pressure for $Cr_{0.995}Re_{0.005}$

The variation of T_N with pressure is shown in the Table. 6.1. It is shown diagrammatically in Figure 6.10. Initially the Neel temperature seems to decrease quite rapidly with pressure at the rate of about 13^o C/kbar. Beyond 1 kbar, it decreases at the slower rate of 2.5 ^{o} C/ kbar. The point marked 'x' in the figure is the triple point . Above this pressure the transition is from the incommensurate antiferromagnetic phase to the paramagnetic phase, while below this pressure ,the transition is from the commensurate to the paramagnetic phase.

According to the two-band model, the Neel temperature variation is described by [10]:

$$k_B T_N = E exp(-1/\lambda) \tag{6.16}$$

where

$$\lambda = \frac{4\gamma^2 V(0) k_c^2}{8\pi^2 v + \gamma^2 V(0)(K^2 + 2Kk_c - 6k_c^2)} \tag{6.17}$$

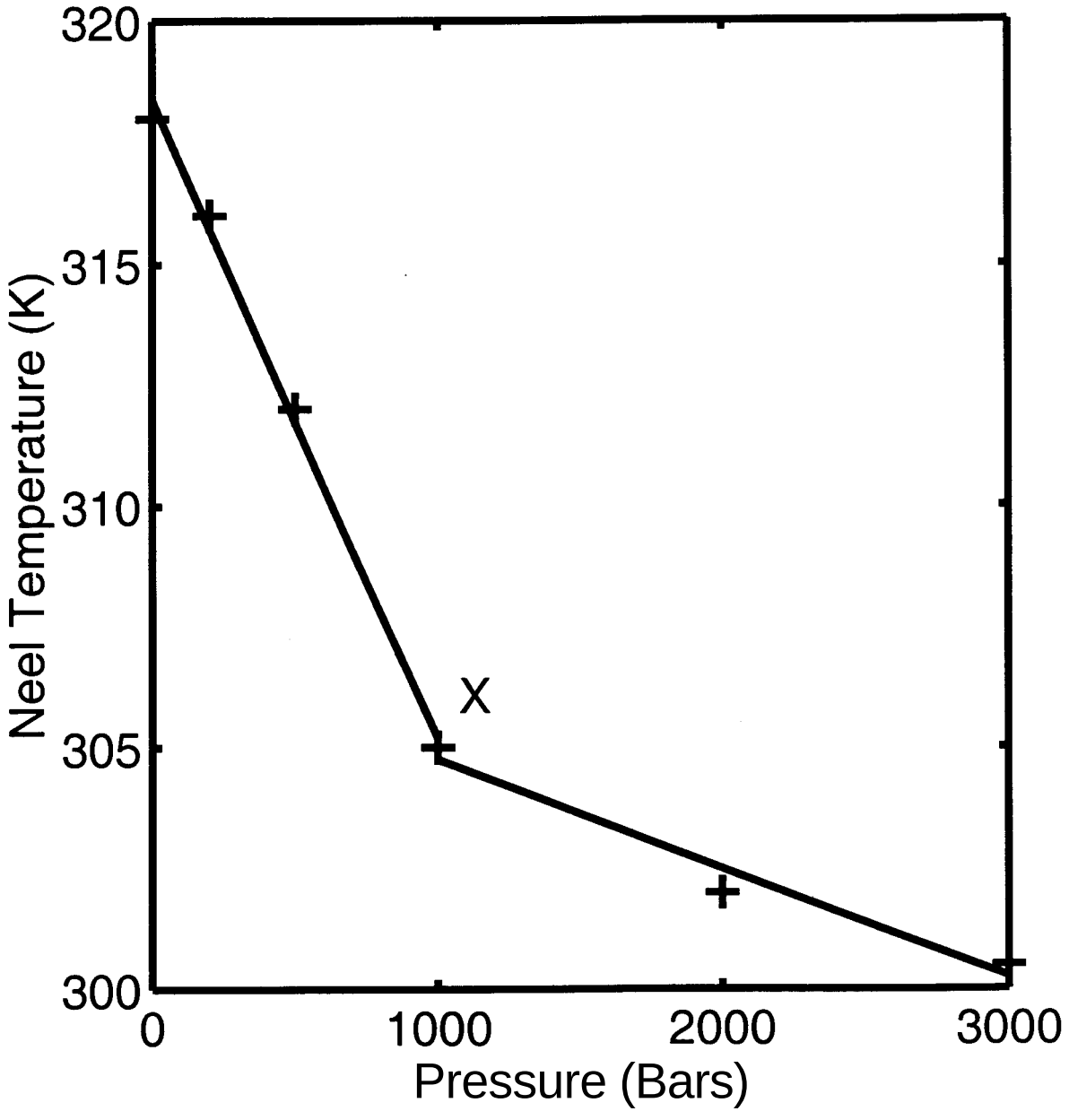

Figure 6.10: Variation of the Neel temperature with pressure in $Cr_{0.995}Re_{0.005}$. Key- 'o'- T_n from Resistivity data, '+' - T_n from Thermopower data

E is the bandwidth of the order of several eV.

V(0) is the average screened coulomb potential.

Since $k_c \sim p^{1/3}$, it is seen from Eq. 6.16 that

$$k_B T_N = E exp(-(p/p_o)^{1/3}) \tag{6.18}$$

where p is the hydrostatic pressure applied on the system and $p_o = 2\pi^2/\gamma^2 V(0)$ is a constant having the dimensions of pressure. The bandwidth E does not vary much with pressure, hence the dominant behaviour will be due to the exponential term.

Since in the incommensurate phase, parts of the Fermi surface have been annihilated, y , which is the matrix element for the overlap between electrons in the same band, will become less and hence ***p,*** will be more in the incommensurate phase. This means that the slope of the T_N vs p curve will be much less in the incommensurate phase.

The theoretical phase diagram for Chromium alloys [11, 12], is shown in Fig. 6.11. The experimental phase diagram (Fig. 6.10) differs from the theoretical prediction in some aspects. Firstly the curvature of the phase boundary between the commensurate (AF,) AFM phase and the paramagnetic phase is not given correctly in the theories of Rice as well as Shibatani. The curvature of the incommensurate-paramagnetic phase boundary fits the theory of Shibatani rather than that of Rice. This is due to the fact that, while the Rice model assumes spherical electron and hole surfaces of different radii, the Shibatani model uses octahedra of different sizes with planar nesting surfaces, with a reservoir of electrons corresponding to the rest of the Fermi surface, which more closely approximates the situation in Cr.

6.2.5 Resistivity results on $Cr_{0.99}Re_{0.01}$

Fig. 6.12 shows the resistivity anomaly for $Cr_{0.99}Re_{0.01}$ as a function of the reduced temperature (T/T_N) for different pressures. It is seen that while the curves for 1 bar, 250 bars and 700 bars overlap one another when plotted as a function of the reduced temperature, the curve at 2 kbar has a prominent 'tail', which extends to well above the Neel temperature.

The other prominent feature of the curves is the dip in the resistivity anomaly on the low temperature side. There have been varying interpretations for the 'dip' in the anomaly at low temperatures. Arajs et al [6] made a thorough study of the resistivity of Cr-Re alloys for various compositions. They speculated that the 'dip'

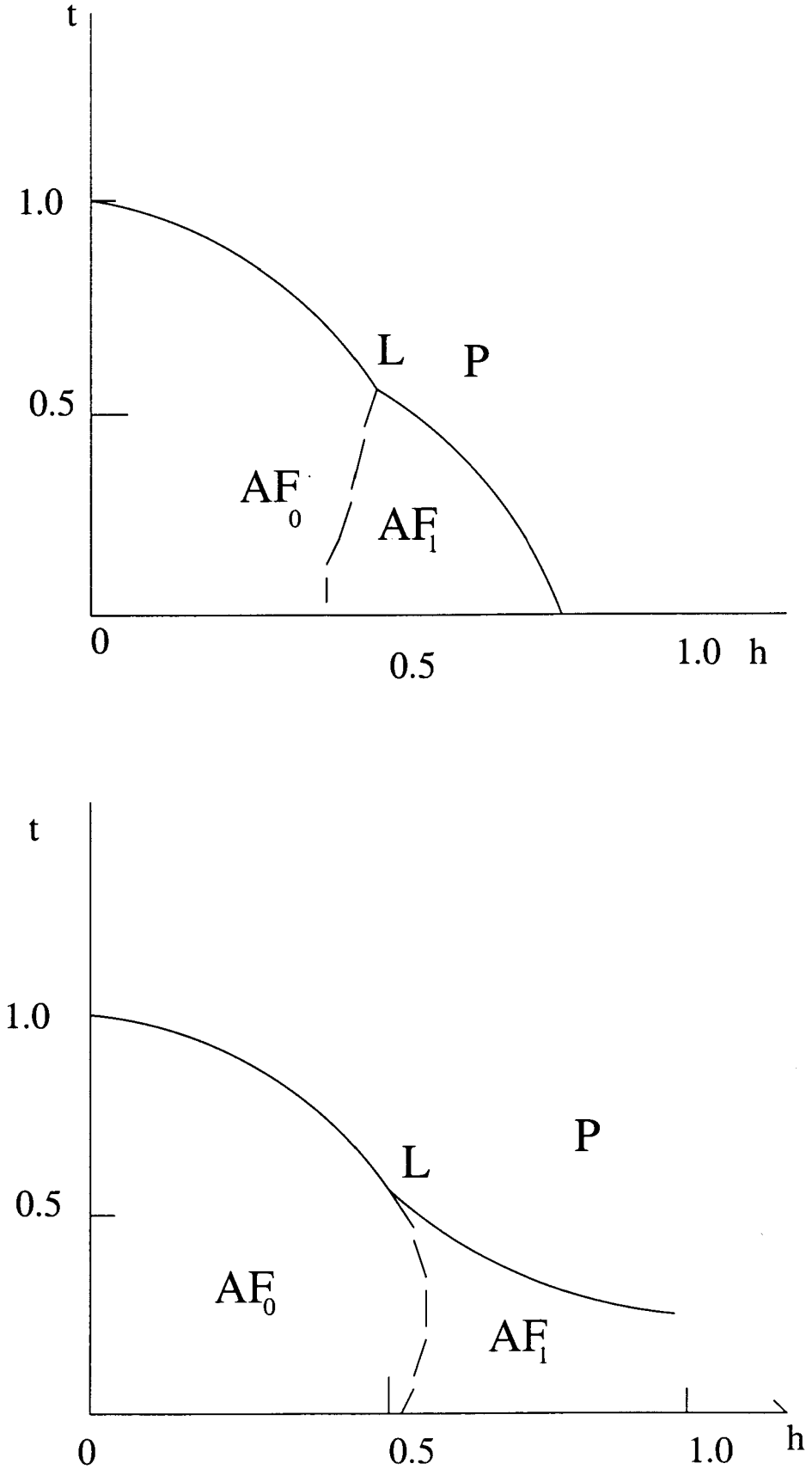

Figure 6.11: Theoretical phase diagrams for Chrornium based on the models of Rice and Shibatani

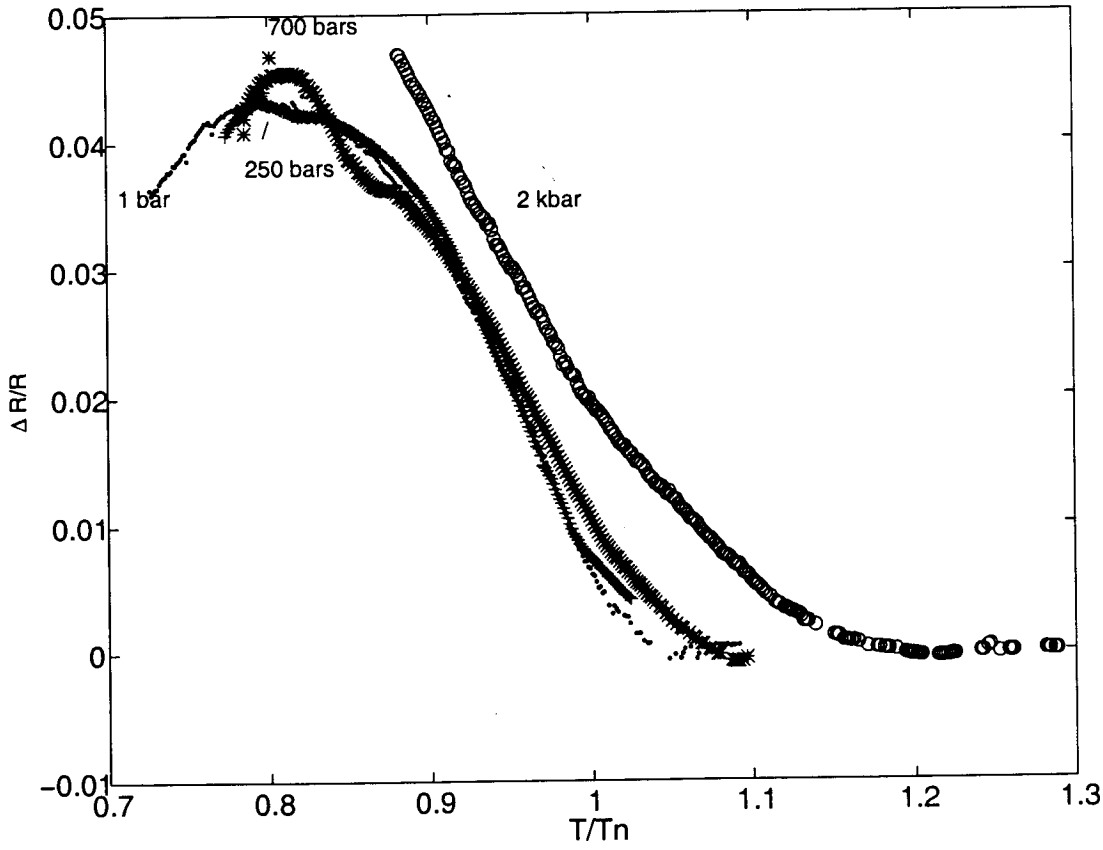

Figure 6.12: Resistivity anomaly in $Cr_{0.99}Re_{0.01}$ as a function of the reduced temperature for different pressures

on the low-temperature end could be due to the fact that due to the annihilation of parts of the Fermi surface, the number of final available states for the scattered electrons is reduced. Since Equation 6.5 takes into account only the reduction in the number of charge carriers, it does not describe the 'dip' in the curve.

Another possibility for the origin of the 'dip' is that at low temperatures, the number of phonons which are available for scattering the electrons is considerably reduced. Hence the linear extrapolation from the paramagnetic phase may not hold good. Hence the correct expression for the extrapolated resistivity should take into account this factor also.

To decide which of the above two factors is predominantly responsible for the 'dip', the resistivity data was analyzed taking both the factors into consideration.

Initially, the data was analyzed according to the procedure given in Section. 6.2.3. The results obtained using this procedure are given in the table below:

Table 6.2: Pressure dependence of the Neel temperature and the energy gap in $Cr_{0.99}Re_{0.01}$

Pressure (bars)	Neel temperature (K)	Energy gap in eV (0 K)	A (0)/kT	β
1	415	0.03	0.84	0.5
250	398	0.023	0.67	0.61
700	386	0.015	0.45	0.55
2000	342	0.014	0.48	0.48

The above table shows that the very sharp decrease of the Neel temperature with pressure for this system as compared to $Cr_{0.995}Re_{0.005}$. The transition temperatures given above maybe in error by ± 1. The error involved in the determination of $\Delta(0)$ could be around ± 0.001. The Neel temperature is shown as a function of pressure in Fig. 6.13

The Neel temperature decreases quite rapidly ($\sim 60°$C/kbar), till 250 bars. At higher pressures, the rate of decrease is much slower ($\sim 30^o$C/kbar). dT_N/dP seems to be much higher in the case of $Cr_{0.99}Re_{0.01}$ than in the case of $Cr_{0.995}Re_{0.005}$. In this case the triple point seems to be around 250 bars and 400 ^{o} C. The exponential dependence of T_N on pressure as seen from Eq. 6.18, is not obvious in Fig. 6.13 or Fig. 6.10. The exponential dependence will be clear only if the measurements are carried out to very high pressures. For example, Mcwhan and Rice [4] have made measurements upto 82 kbars. In the present work, the phase boundaries could not

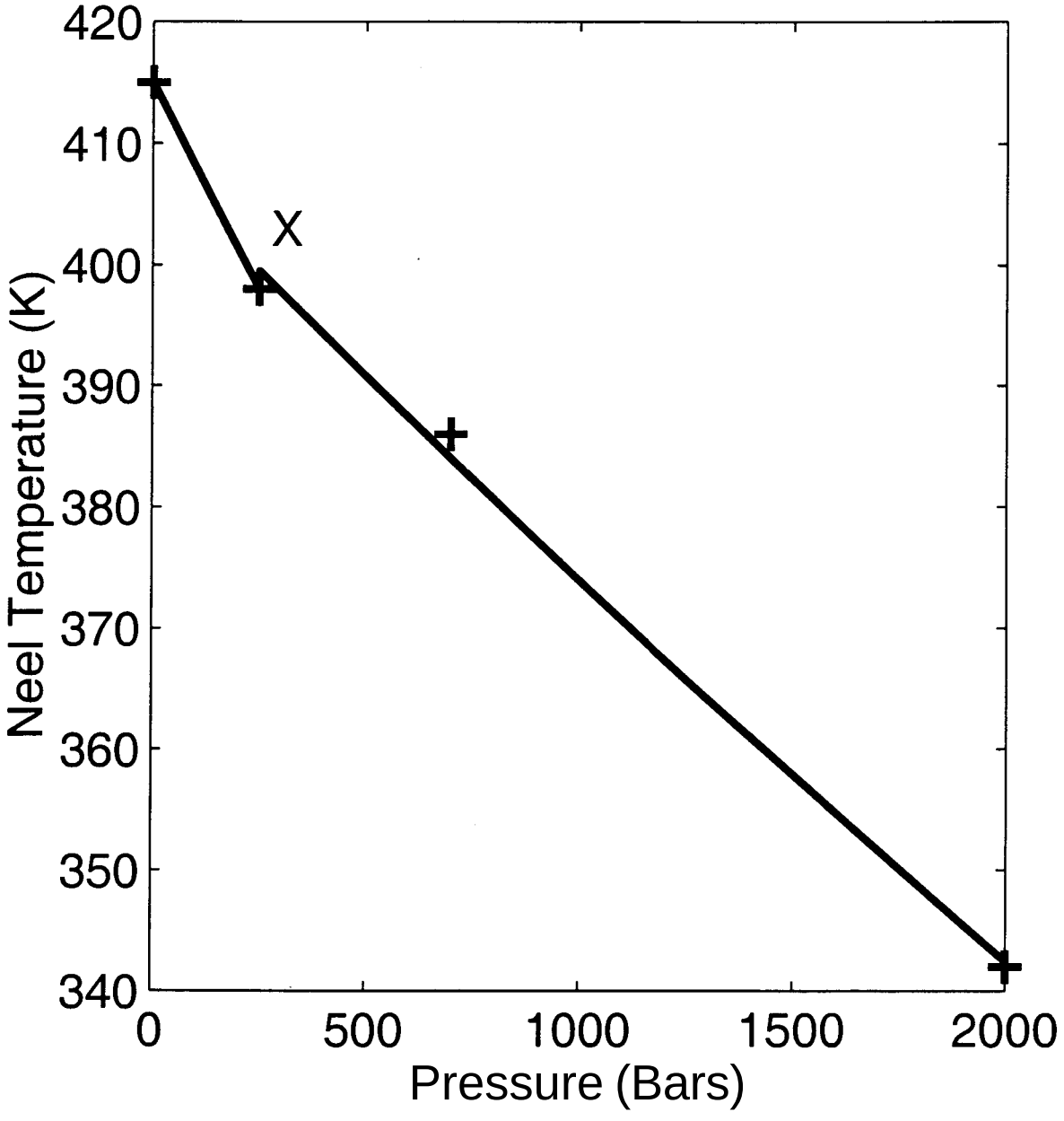

Figure 6.13: Variation of the Neel temperature with pressure in $Cr_{0.99}Re_{0.01}$

be tracked to pressures higher than a few kbars, since at these high pressures the transition temperatures become less than the room temperature.

Differentiating Eq. 6.18, we obtain

$$\frac{dT_N}{dp} = -\frac{E}{3}\left(\frac{p}{p_o}\right)^{2/3} \exp -(p/p_o)^{1/3} \tag{6.19}$$

This has been obtained by neglecting the variation of E with pressure. It is seen from this equation that dT_N/dp depends crucially on E as well as p_o. Since E will increase with increase in electron concentration, dT_N/dp is higher for $Cr_{0.99}Re_{0.01}$ than $Cr_{0.995}Re_{0.005}$.

6.2.6 Temperature variation of the resistivity anomaly in $Cr_{0.99}Re_{0.01}$

A more rigorous analysis than that described in Sec. 6.2.3 was attempted by taking into account both the reduction in the density of d- states , as well as the reduction in the number of phonons available for scattering the electrons.

The reduction in the density of final states is taken into account in the following manner: If σ_n/σ_{np} is the relative change in the conductivity as given by Equation 6.5, then the correct expression for the change in the conductivity will involve the change in the relaxation time.

The complete expression for the resistivity anomaly, taking into account the change in the relaxation time is given by:

$$\frac{\Delta R}{R} = f\left[\left(\frac{1}{f} - 1\right)\left(1 - \frac{\tau_a}{\tau_p}\right) + 1 - \frac{\sigma_n}{\sigma_{np}}\frac{\tau_a}{\tau_p}\right] \tag{6.20}$$

Where τ_a and τ_p are the relaxation times in the antiferromagnetic phase and the paramagnetic phase respectively.

This formula is obtained by modifying Eq. 6.6. In the original calculation of Mcwhan and Rice, the change in conductivity is assumed to be solely due to the change in the number of charge carriers. If we the take the relaxation times to be different in the two phases Eq. 6.6 gets modified to

$$\frac{\Delta R}{R} = \frac{(\sigma_{np} + \sigma_{rp})\tau_p - (a, + \sigma_{rp})\tau_a}{(\sigma_n + \sigma_{rp})\tau_a} \tag{6.21}$$

Simplifying the above equation we obtain Eq. 6.20.

The relaxation times in the transition metals are generally inversely proportional to the density of d-states at the Fermi level [13].

$$\tau \sim \frac{1}{N_d} \tag{6.22}$$

If N_d is the density of d-states in the paramagnetic phase, the density of states in the antiferromagnetic phase will less than this, since an energy gap is introduced at the fermi surface. If g is the fraction of the Fermi surface which has condensed (Eq. 6.8), then

$$\tau_a = (1-g)N_d + gN_d\frac{n_\Delta(T)}{n(T)} \tag{6.23}$$

$$\tau_p = N_d \tag{6.24}$$

Here n_Δ and n are the number of phonons which have an energy greater than the energy gap, and the total number of phonons at a temperature T respectively. The number n_Δ enters in to the calculation since only that fraction of phonons which have energy greater than Δ can scatter the electrons across the energy gap.

Substituting Eq. 6.23 and Eq. 6.24 into Eq. 6.20, we obtain, the expression for the resistivity anomaly which takes into account the change in the relaxation time.

The total number of phonons at a temperature T is given by [14]

$$n(T) = \int_0^{\omega_D} d\omega \frac{3V}{2\pi^2 v^3}\frac{\omega^2}{e^{\frac{\hbar\omega}{k_B T}} - 1} \tag{6.25}$$

The number of phonons with an energy greater than A is given by:

$$n_\Delta = \int_{\Delta/\hbar}^{\omega_D} d\omega \frac{3V}{2\pi^2 v^3}\frac{\omega^2}{e^{\frac{\hbar\omega}{k_B T}} - 1} \tag{6.26}$$

Where V is the volume and v is the velocity of the phonons. However these factors are not involved in 'the final calculation, since Eq. 6.20 involves only the ratio of Eq. 6.25 and Eq. 6.26. Here w is the frequency of a phonon and ω_D is the Debye frequency. The Debye temperatures for $Cr_{0.99}Re_{0.01}$ and $Cr_{0.995}Re_{0.005}$ have been taken as 630 K [15], which is the Debye temperature for pure Chromium. The Debye frequency is calculated from the Debye temperature, using the equation:

$$\omega_D = k_B\theta_D/\hbar \tag{6.27}$$

The integrals in Eq. 6.5, Eq. 6.25 and Eq. 6.26 were evaluated numerically.

In using Eq. 6.20 to explain the resistivity anomaly, we have assumed that β is equal to 0.5 in Eq. 6.10. The deviation of the values of β should be due to the variation of the relaxation time , which is being accounted for in Eq. 6.20.

However it was found that taking into account the change in the density of available states does not make much of a difference. This is because the ratio $\frac{n_\Delta(T)}{n(T)}$ does not change much over the temperature range 300 K to 420 K, which is the temperature range of our interest. Over this temperature range, this ratio changes from 0.96 to 1.00. Hence this does not explain the sudden 'dip' in the resistivity anomaly.

To check whether the change in the number of phonons is important, this factor was also taken into account.

The expression for the resistivity taking into account the phonon scattering is given by [9]:

$$\rho = \frac{C}{M\theta_R}\left(\frac{T}{\theta_R}\right)^5 \int_0^{\theta_R/T} \frac{z^5 dz}{(e^z - 1)(1 - e^{-z})} \tag{6.28}$$

At high temperatures ($\sim \theta_D$) the integral in the above equation will reduce to $\frac{1}{4}\left(\frac{\theta_R}{T}\right)^4$, hence the resistivity will vary linearly with temperature. At low temperatures the resistivity varies as T^5.

Experimentally it has been proved in most cases that θ_R is nearly equal to θ_D, the Debye temperature [9]. Ideally the electrons are scattered by only the longitudinal lattice vibrations [9, 16]. In this case θ_l, which is the temperature characterizing the longitudinal vibrations, is about 50% to 100% more than θ_D.

The disagreement between the theoretical result and the experimental curve is brought out in Fig. 6.14

In case we use θ_l in our calculations instead of θ_D better agreement might be possible between experiment and theory.

6.3 Thermopower studies on Cr-Re alloys

6.3.1 Experimental

Thermopower of $Cr_{0.995}Re_{0.005}$ and $Cr_{0.99}Re_{0.01}$ alloys was measured in the temperature range 25^o C to 100 ▪ C using the differential method. This method has been described in detail in chapter 2. The Teflon cell is used in the case of Chromium alloys.

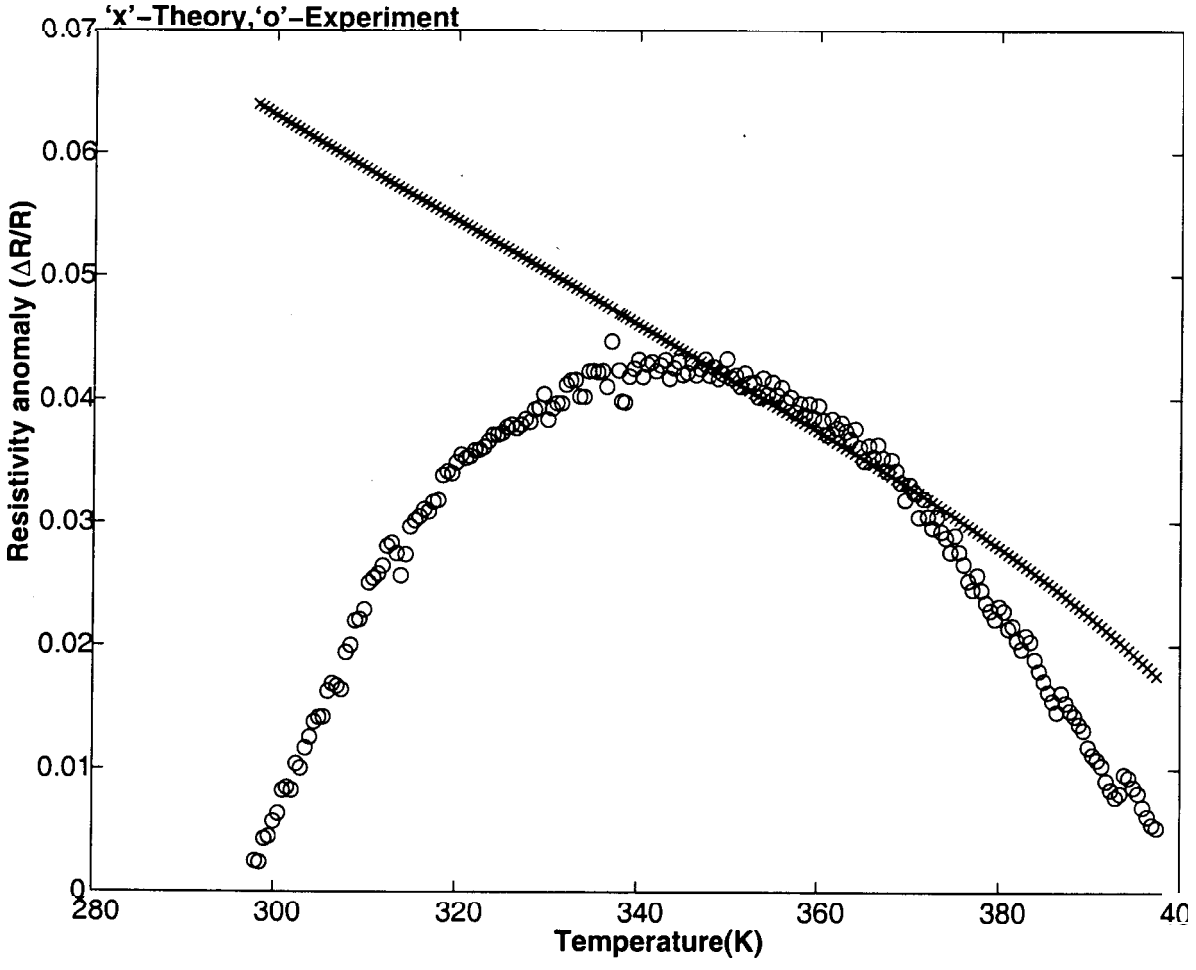

Figure 6.14: Variation of the resistivity anomaly as given by the theory and by experiment in $Cr_{0.99}Re_{0.01}$, key :- 'x' - Theory, 'o'- Experiment

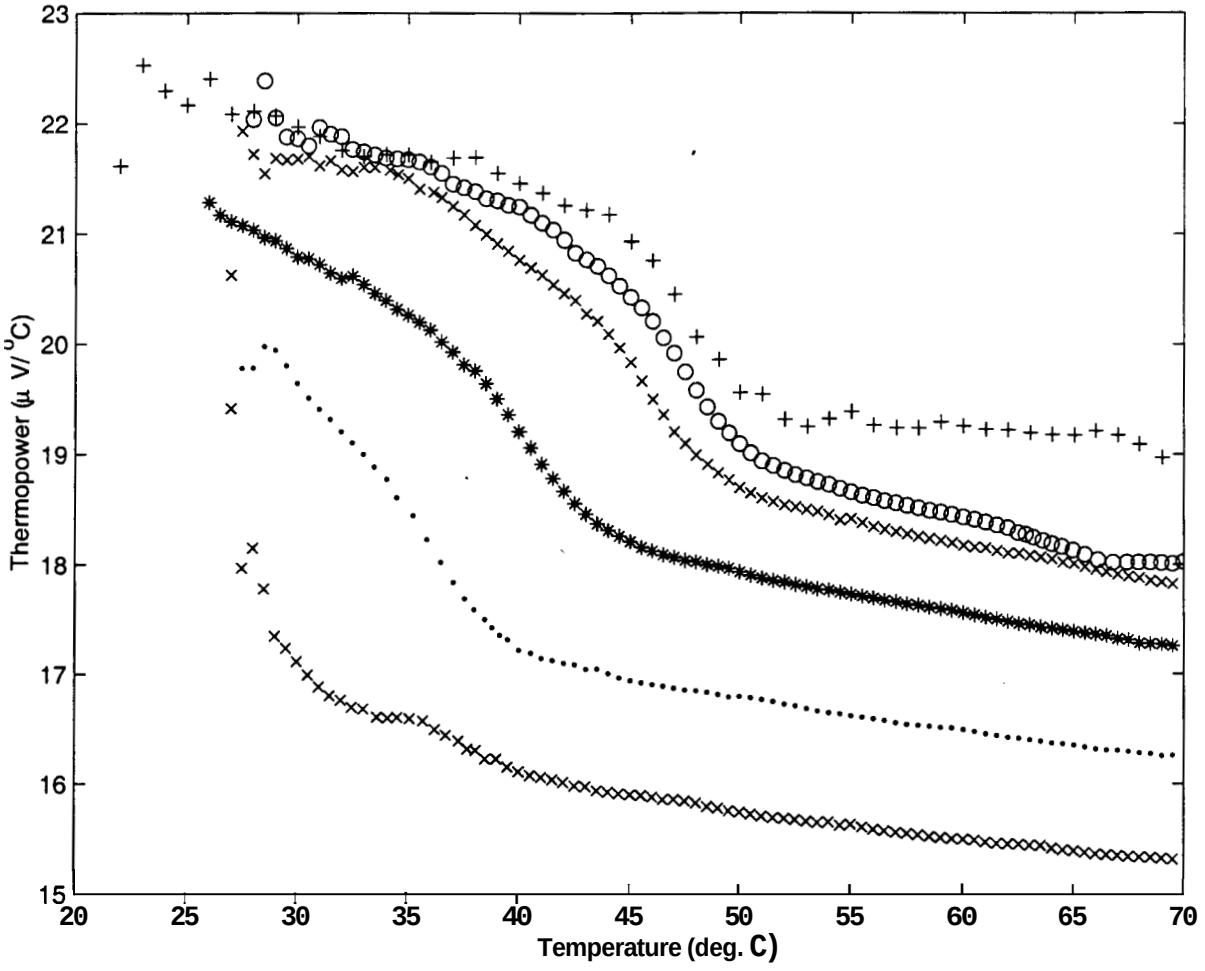

Figure 6.15: Thermoelectric power of $Cr_{0.995}Re_{0.005}$ as a function of temperature at different pressures. key:- '+' - 1 bar, 'o'- 200 bars, 'x' - 500 bars, '*' - 1 kbar, '.' - 2 kbars, 'X' - 3kbars

---

In this method Chromel-Alumel thermocouple wires are spot-welded at the two ends of the sample. The sample, which is in the form a thin flake is mounted vertically in a Teflon cell. Silicone oil was used as the pressure transmitter for the high pressure studies.

6.3.2 Results and Discussion

The thermopower is shown as a function of temperature for pressures ranging from 1 bar to 3 kbar in Fig. 6.15.

From the figure it is seen that the antiferromagnetic to the paramagnetic phase manifests as a decrease in the thermoelectric power. Another easily-noticeable fea-

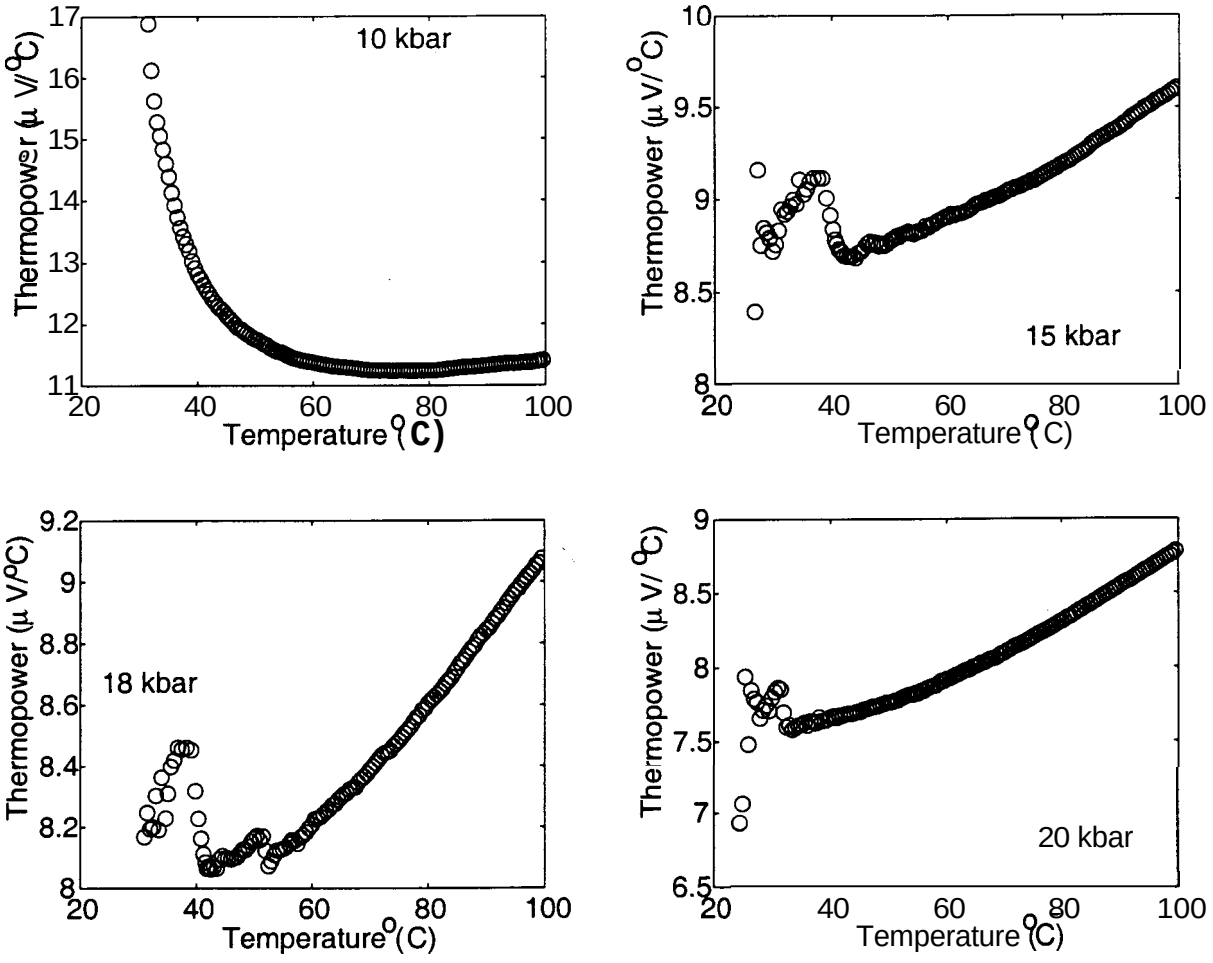

Figure 6.16: Thermoelectric power of $Cr_{0.995}Re_{0.005}$ as a function of temperature at different pressures.

ture is that the thermopower at a given temperature decreases with pressure.

The thermopower for pressures in the range 10 k to 20 kbars is given in Fig. 6.16.

It is seen from Fig. 6.16, that for pressures greater than 10 kbar, the thermopower in the paramagnetic phase has a positive slope , in contrast to the negative slope at lower temperatures. The TEP for Cr changes to a positive slope even at atmospheric pressure. However this happens only at temperatures higher than 400 K. Since the measurements reported here are only for temperatures lower than that, the change of slope is not observed in this case. The continued decrease in the TEP beyond the actual Neel temperature is due to the persistence of magnetic order. For high pressures , the Neel temperature is much lower than the room temperature and hence the change to a positive slope in the TEP occurs at around room temperature

We try to explain the thermopower results using Mott's expression. The expression for diffusion thermoelectric power, according to Mott [13] is given by:

$$S_{diff} = \frac{\pi^2 k_B^2 T}{3e} \frac{dIn\sigma}{dE}|_{E=E_F} \tag{6.29}$$

Eq. 6.29 can also be written as:

$$S_{diff} = \frac{\pi^2 k_B^2 T}{3e} \left[\frac{\partial In\sigma}{\partial E}\right]_{E_F} \tag{6.30}$$

$$\sim \frac{\pi^2 k_B^2 T}{3e} \left[\frac{\partial In\Sigma}{\partial E} + \frac{\partial Inl}{\partial E}\right]_{E_F} \tag{6.31}$$

Where Σ is the area of the Fermi surface and 1 is the average mean free path over C. In an AFM Cr alloy, Σ is the area of the Fermi surface which has not condensed, which might in some cases be quite sensitive to the energy E. In the temperature region of interest below the Neel temperature T_N, where the resistivity anomaly is seen, the contribution of the second term may be large when electron-phonon scattering largely determines the mean free path.

The mean free path is related to the relaxation time by the equation:

$$l = \tau v \tag{6.32}$$

Trego and Mackintosh [18] discussed a model in which the energy gap 2A increases from a value much smaller than the characteristic energy E_{ph} of the phonon, to a value A $>$ E_{ph}, and showed that $(d\tau_{ph}/dE)_{E_F}$ exhibits a maximum when A $\sim$ E_{ph}. This should give a positive maximum in the temperature dependence of S. Since measurements have not been made at temperatures below the ambient, the maximum in the TEP, is not seen in Fig. 6.15. However the energy gap obtained $(\sim 0.03eV)$ for $Cr_{0.99}Re_{0.01}$ at atmospheric pressure is consistent with a maximum around room temperature (since 300 k $\sim$ 0.025 eV).

The model of Trego and Mackintosh [18] therefore relates the anomalies in the TEP to the density of states (DOS).

In contrast to this the work of Schroder, Yessik and Baum seems to suggest that the term $dInN_d/dE$, does not contribute much to the thermopower. This can be related to the fact the density of states has a minimum near the Fermi energy for Cr. Since the density of states has a minimum dN_d/dE is very small , but since N_d is also small, $\frac{1}{N_d}\frac{dN_d}{dE}$ could still be substantial near E_F.

Schroder et al [19] say that the predominant contribution to the TEP comes from the term $dIn\Sigma/dE$. Schroder et al reached this conclusion after performing a detailed study on Cr-Fe alloys. The DOS curve increases rapidly with Iron concentration and reaches a sharp maximum at $Fe_{19}Cr_{81}$. One would expect that the TEP would change rapidly near $Fe_{19}Cr_{81}$. However the experiments show that the TEP is nearly constant for the alloys with 15% to **23%** Fe.

This conclusion can also be reached looking at the TEP for all the Cr alloys. Since some of the Cr alloys increase the electron concentration and some decrease it, the Fermi energy might lie on either side of the minimum in the DOS. Therefore the thermopower should change sign when E_F crosses the minimum. However this change in sign is not observed for any of the Chromium alloys studied till date.

This is a proof that the DOS is not the only factor which determines the TEP. It should be noted that $d\Sigma/dE$ is negative (which gives a positive sign for TEP), for the d-states.

We define a TEP anomaly ,which is similar to the resistivity anomaly. The TEP is defined as the difference between the TEP in the AFM phase and the linear extrapolation of the TEP from the paramagnetic phase divided by the TEP in the AFM phase. The TEP anomaly is shown in Fig. 6.17.

It is seen from Fig. 6.17, that the magnitude of the TEP anomaly , unlike the resistance anomaly, does not decrease with pressure. On the contrary, there is a slight increase in the magnitude of the anomaly with increasing pressure. Hence it is possible to track the transition to very high pressures. This makes TEP a better probe than resistivity to track the variation of T_N with pressure. The shift in T_N with increase in pressure is clearly seen in the TEP anomaly.

6.3.3 Thermopower of $Cr_{0.99}Re_{0.01}$

Fig. 6.18 shows the thermoelectric power for $Cr_{0.99}Re_{0.01}$ for pressures ranging from 200 bars to 1.5 kbars.

The TEP at a particular temperature, decreases with increase in pressure. There is no marked change in the TEP at T_N, unlike the case of $Cr_{0.995}Re_{0.005}$. As in the case of $Cr_{0.995}Re_{0.005}$, the TEP shows a positive slope in the paramagnetic phase at higher pressures (Fig. 6.19. However, it is surprising that the thermopower anomaly in this case is less distinct than in the case of $Cr_{0.995}Re_{0.005}$

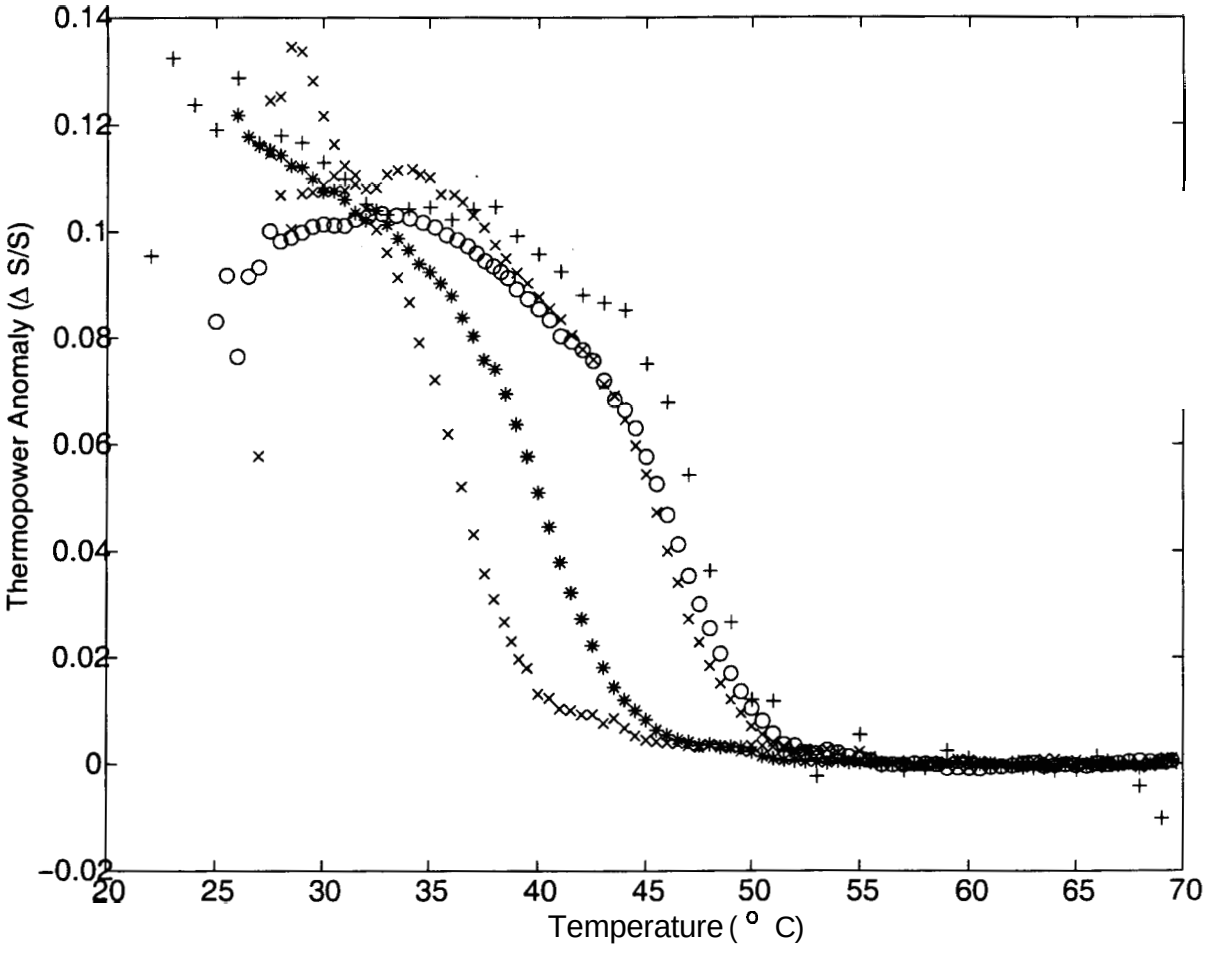

Figure 6.17: Anomaly in the Thermoelectric power of $Cr_{0.995}Re_{0.005}$ as a function of temperature at different pressures. key:- '+' - 1 bar, 'o'- 200 bars, 'x' - 500 bars, '*' - 1 kbar, 'X' - 2 kbars

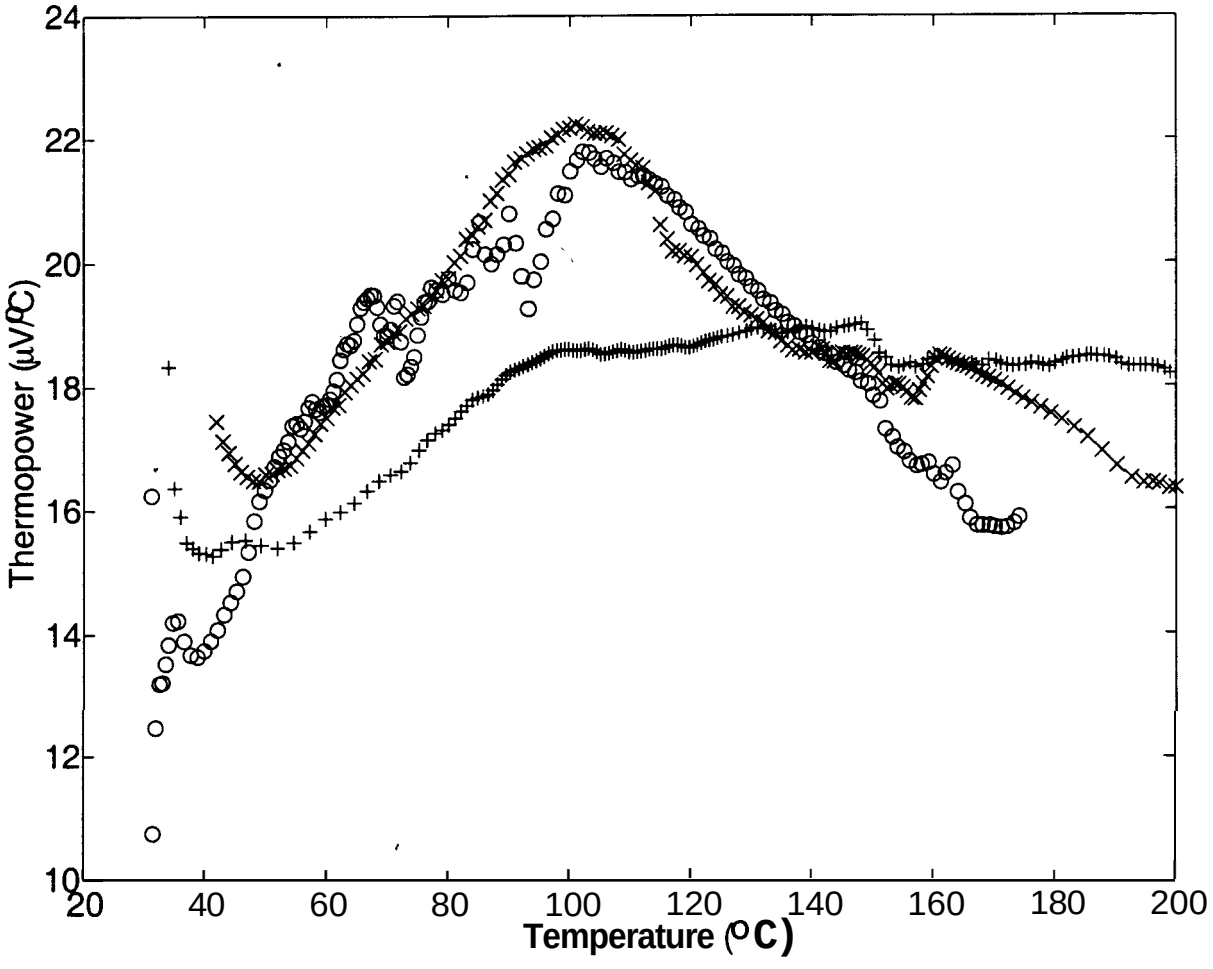

Figure 6.18: Thermoelectric power of $Cr_{0.995}Re_{0.01}$ as a function of temperature at different pressures. key:- 'o'- 200 bars, 'x' - 1 kbar, '+' - 1.5 kbars

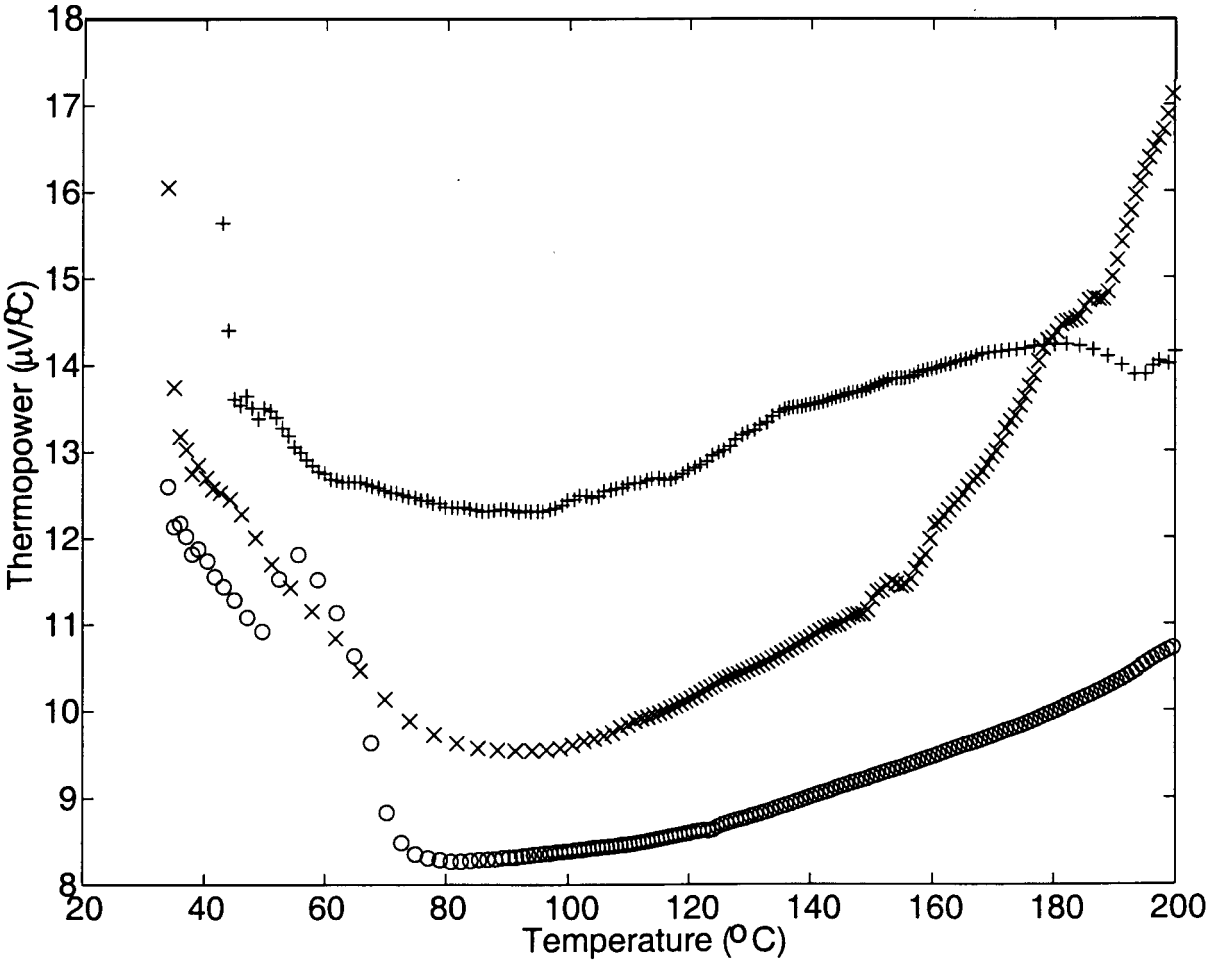

Figure 6.19: Thermoelectric power of $Cr_{0.995}Re_{0.01}$ as a function of temperature at different pressures. key:- '+'- **2** kbars, 'X' - **3** kbars, 'o' - 4.5 kbars

6.4 Thermal properties of Cr alloys

Thermal properties of Cr alloys can give us information about the energy levels in the alloy and also about the nature of the transition. Fig. 6.20 shows the specific heat of $Cr_{0.995}Re_{0.005}$ in the temperature range 25^o C to 70^o C. The Neel temperature for this alloy is 45^o C as obtained from the resistivity studies. The specific heat curve shows a peak around 40^o C. Below the transition point, an exponential dependence of the form

$$C_v = A \exp(-2\Delta/kT) \tag{6.33}$$

would have been expected, due to the presence of the energy gap of magnitude 2A. This exponential dependence has been observed below T_c in the case of superconductors which are a very similar system. Fig. 6.20 does not show this exponential dependence below T_N. This might be due to the fact that in Chromium alloys unlike in the case of superconductors, the energy gap is only along a particular direction in k-space.

In the case of a superconductor, the transition is found to be mean field in nature. The specific heat accordingly shows a finite discontinuity at T_c. In the case of Chromium alloys, the behaviour is not very clear from Fig. 6.20. Theoretically we can calculate the region over which mean field behaviour is valid. According to the Ginzburg criterion given in chapter 1,

$$t_G = \frac{k_B^2}{32\pi^2(\Delta C_v)^2\xi_o^2} \tag{6.34}$$

Where t_G is the value of the reduced temperature below which mean field theory is not valid. Since in the case of Chromium and its alloys, the antiferromagnetism is due to itinerant electrons, we can assume the interaction distance ξ_o to be the mean free path of the electrons. This is approximately 30 $\mathring{A}$ in the case of Chromium at 300 K. The change in the specific heat at the transition is $\sim$ 16,000 J/m^3/K (Fig. 6.20). Substituting these values in Eq. 1.22, we obtain $t_G \sim 3 \times 10^{-8}$. Since $T_N \sim$ 300 K, this gives T – $T_N \sim 10^{-5}$ as the temperature within which mean field theory should be valid.

This result highlights an important fact about how the nature of the interaction affects the nature of the transition. If the interaction is only between nearest neighbors, ξ_o will be of the order of order of interatomic distances. Hence mean field behaviour is violated to a greater extent in this case.

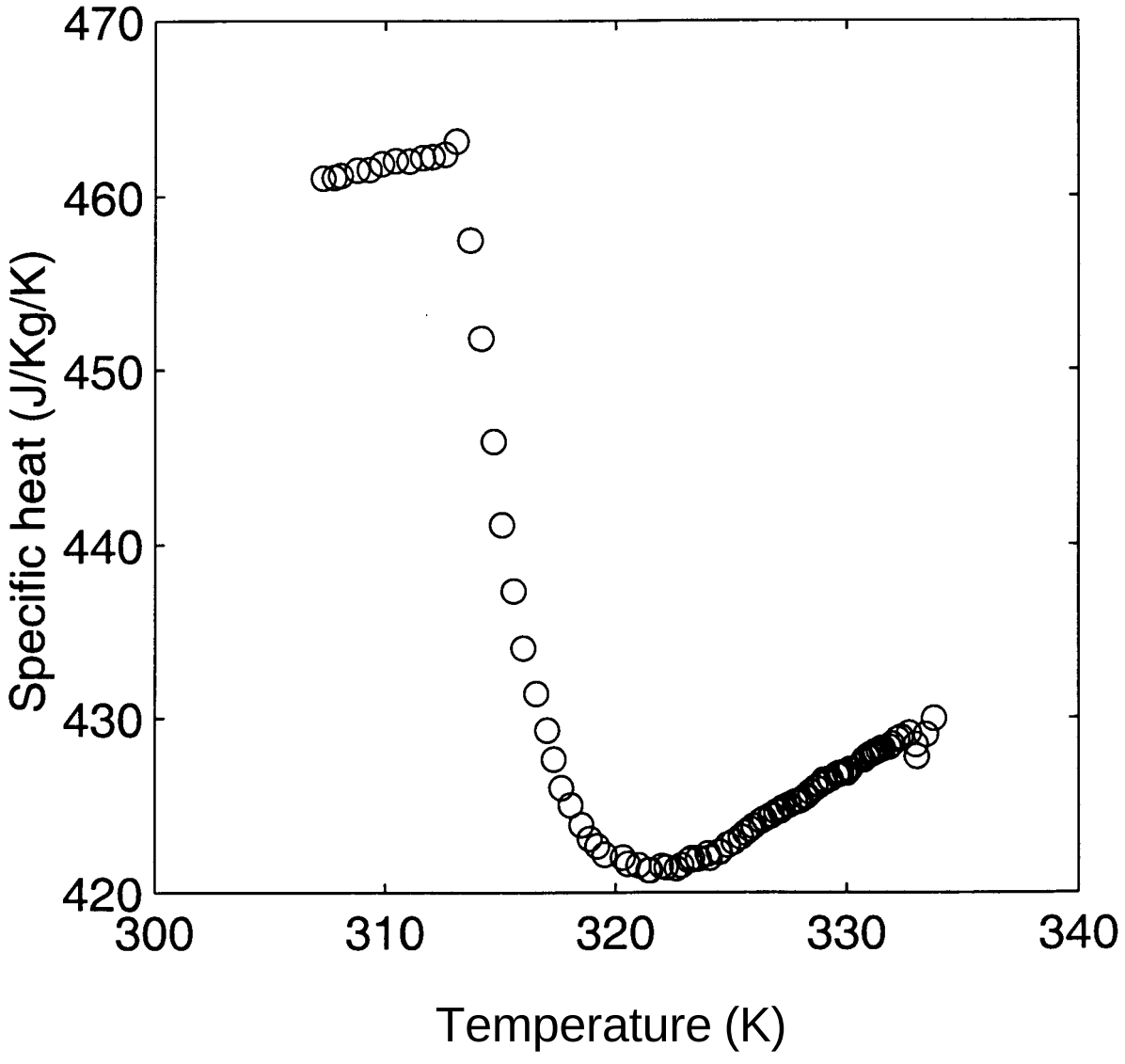

Figure 6.20: Specific Heat of $Cr_{0.995}Re_{0.005}$ at atmospheric pressure

To illustrate this idea we take the case of the Curie point transition in Nickel, discussed in chapter 3. The ferromagnetism in Nickel is supposed to obey the Heisenberg model. The specific heat change at the transition is 6.1034 x 10^5 J/m^3/K. If we assume only nearest neighbour interaction between the spins, the Ginzburg temperature, t_G = 0.002. Since T_C in this case is 631 K, the range over which mean field behaviour is violated is $\sim T_c \pm 1.4K$. Experimentally it is found that the range over which the data fits the non-mean field exponent of -0.1 is $T_c \pm 10$ K. This seems to indicate that even though there is evidence to show that the magnetism in Nickel is also itinerant in character, the critical behaviour of Nickel is consistent with a localized spin model.

6.5 Conclusions

The transition from the antiferromagnetic phase to the paramagnetic phase in Cr-Re alloys is quite clearly seen in both the transport properties, as well as in the thermal properties. The exponents determined for the order parameter, as well as the specific heat are consistent with the mean field nature of the transition. The exponent β for the order parameter variation, was extracted from the resistivity data using the two-band model of Fedders and Martin. This model does not describe the variation of the resistance over the entire range. It fails to predict the anomalous decrease in the resistance at low temperatures. The conventional explanations for this effect, namely, the reduction in the DOS, and the reduction in the number of phonons, also are not able to account for this anomalous decrease. This has been proved using a detailed quantitative analysis of the resistance data. The transition at T_N is seen as a marked decrease in the thermopower. A thermopower anomaly can be defined on the same lines as the resistivity anomaly.

References

[1] H.Umebayashi, G.Shirane,B.C.Frazer and W.B.Daniels, J.Phys.Soc.Jpn, 24. 368 (1968)

[2] Overhauser, Phys.rev, 128, 1437, (1962)

[3] Falicov and Penn, Phys.Rev.; 158 **(2)**, 476, (1967)

[4] Mcwhan,D.B and T.M. Rice, Phys.Rev.Lett, 19, 867 (1967)

[5] E. Fawcett et al, Rev.Mod.Phys, **66(1)**, 25, (1994)

[6] S.Arajs, C.A.Moyer and D.Abukay, phys.stat.sol.(b) 101, 63 (1980)

[7] T.M.Rice, A.Jayaraman and D.B.McWhan, J.Phys(Paris)Colloq.**32**, C1-39(1971)

[8] V.Shubha and T.G.Ramesh, High temp.High Press., 18,311 (1986)

[9] G.T. Meaden, Electrical Resistance of Metals, Clarendon Press, (1965)

[10] P.A.Fedders and P.C.Martin, Phys.Rev, 143, 245, (1966)

[11] T.M.Rice, Phys.Rev.B, **2**, 3619 (1970)

[12] A.Shibatani, A.K.Motozuki and T.Nagamiya, Phys.Rev.,**177**, 984 (1969)

[13] N.F.Mott, Proc.Roy.Soc.Ser **A156**, 368 (1936)

[14] C. Kittel, Introduction to Solid State Physics, 3rd Edition, Wiley Eastern (Pvt Ltd), New Delhi, (1971)

[15] N.W.Ashcroft and N.D.Mermin, Solid State Physics, Holt,Rinehart and Winston, 1976

[16] Blackman, Proc.Phy.Soc.A,**64** 681 (1951)

[17] R.D. Barnard in Thermoelectricity *in* Metals and Alloys, Taylor and Francis LTD. 1972

[18] A.L.Trego and A.R.Mackintosh, Phys.Rev., 166, 495 , (1968)

[19] Schroder,Yessik and Neal Baum, J.App.Phys.,**37(3)**, 1019,(1966)